Student thesis series INES nr 500

ENSO teleconnections – Analysis of time lag between tropical Pacific sea surface temperature and climate and vegetation anomalies

Jiří Navrátil

2020
Department of
Physical Geography and Ecosystem Science
Lund University
Sölvegatan 12
S-223 62 Lund
Sweden

Jiří Navrátil (2020).
ENSO teleconnections – Analysis of time lag between tropical Pacific sea surface temperature and climate and vegetation anomalies
ENSO fjärrpåverkan – Analys av tidsfördröjning mellan tropiska stilla havets yttemperatur, klimat och vegetationsavvikelser
Master degree thesis, 30 credits in *Physical Geography and Ecosystem Analysis*
Department of Earth and Ecosystem Sciences, Physical Geography and Ecosystem Science, Lund University

Level: Master of Science (MSc)

Course duration: *January* 2018 until *January* 2020

ENSO teleconnections – Analysis of time lag between tropical Pacific sea surface temperature and climate and vegetation anomalies

---

Jiří Navrátil

Master thesis, 30 credits, in *Physical Geography and Ecosystem Analysis*

Thomas Holst
Department of Physical Geography and Ecosystem Science,
Faculty of Science, Lund University, Sweden

Lars Eklundh
Department of Physical Geography and Ecosystem Science,
Faculty of Science, Lund University, Sweden

Examiners:
Martin Berggren, Department of Physical Geography and Ecosystem Science,
Faculty of Science, Lund University, Sweden
Mayra Rulli, Department of Physical Geography and Ecosystem Science,
Faculty of Science, Lund University, Sweden

Acknowledgements

I would like to thank:

(i) Isabel Rasmussen Vinterbladh for the very appreciated help with programming which made the processing of large amounts of data much smoother and faster.

(ii) My supervisors Thomas Holst and Lars Eklundh for supervising this project and most importantly for tolerance and endless patience with me.

(iii) Ellen Carneheim for the Swedish title of the thesis and help with proof-reading the manuscript.

(iv) Martina Nováková and Lone Mokkenstorm for helpful advice on the software used in this project.

(v) My whole family for support and especially my parents for financially supporting me during the work on this project.

Abstract (English)

El Niño-Southern Oscillation (ENSO) affects weather and climate in regions spread all around the Earth via teleconnections. While quite a lot of research has been done on recognizing what regions are affected by these and what is the sign of the associated temperature, rainfall and vegetation anomalies, not that much attention has been paid to the timing of the impacts with respect to the ENSO state. This project found that the ENSO-caused anomalies were never at their peak simultaneously with an ENSO event culmination for any of the three examined variables – precipitation, temperature and normalized difference vegetation index (NDVI) – in any of the eight study areas. It was also found that there is no seasonally uniform time lag between sea surface temperature (SST) anomalies in tropical Pacific and the associated anomalies in a specific region. On the contrary, the anomalies are generally strongest in late northern hemisphere spring to early northern hemisphere summer for all the variables in all the regions and that they are mainly affected by the ENSO state in the preceding northern hemisphere summer and northern hemisphere winter. Since these findings were not expected in comparison with studies already published, it seems necessary to test the time lag between tropical Pacific SST and impacts of ENSO teleconnections in more studies with possibly diverse methodologies before drawing conclusions that would revise the so far published knowledge about the timing of ENSO teleconnections impacts as suggested by the results of this study.

Abstrakt (čeština)

El Niño-Jižní oscilace (ENSO) ovlivňuje počasí a podnebí v oblastech rozprostřených po celém světě skrz dálkové vazby. Zatímco existuje mnoho studií věnujících se identifikaci těchto oblastí a znaménku souvisejících odchylek teploty, srážek a vegetace, ne mnoho pozornosti bylo dosud věnováno načasování zmíněných odchylek s ohledem na stav ENSO. Tato studie ukázala, že odchylky ani jedné ze zmiňovaných veličin – teploty, srážek a vegetačního indexu NDVI – nikdy nekulminovaly současně s kulminací jedné z fází ENSO (El Niño či La Niña) v žádné ze zkoumaných studijních oblastí. Zároveň nebylo nalezeno žádné zpoždění mezi povrchovou teplotou moře (SST) v tropickém Tichém oceánu a souvisejícími odchylkami v určitém regionu, jež by bylo zřejmé ve všech ročních obdobích. Naopak bylo zjištěno, že tyto odchylky všech zkoumaných proměnných jsou ve všech zkoumaných oblastech většinou největší v pozdním jaru a brzkém létě severní polokoule a že jsou způsobené hlavně stavem ENSO v předcházejícím létě a zimě severní polokoule. Vzhledem k tomu, že tyto výsledky nebyly v porovnání s již publikovanými studiemi očekávané, zdá se být nezbytné nejprve otestovat zpoždění dopadů dálkových vazeb ENSO za SST v tropickém Pacifiku ve vice studiích (s případně odlišnými použitými metodami) než vyvozovat závěry, které by pozměňovaly dosud publikované poznatky o načasování dopadů dálkových vazeb ENSO tak, jak by navrhovaly výsledky této práce.

Table of contents

1 Introduction

El Niño-Southern Oscillation (ENSO) has been one of the most frequent topics in scientific literature about inter-annual climate variability. It affects both human and natural systems such as agriculture and forestry, fisheries, public health, both marine and terrestrial ecosystems and the global carbon as well as hydrological cycle (Yeh et al., 2018). Compared to other climate phenomena, ENSO is special not only due to its strong presence and a degree of predictability in the tropical Pacific, but also the worldwide impact it has on weather via atmospheric teleconnections (McPhaden et al., 2006). Among other effects, ENSO also impacts primary productivity of terrestrial ecosystems ranging from tropical rainforests to northern hemisphere forests, mostly by modulating precipitation, surface temperature and sunlight availability via regulating cloudiness (McPhaden et al., 2006).

There are still certain aspects that have not yet been fully explored and need further research from which societies could significantly benefit since seemingly disconnected sectors, with public health and agriculture given here as the most prominent examples, are tightly linked to ENSO events. For instance, El Niño 1997/98 caused 22 000 death tolls, most of which are accounted for ENSO-related disease outbreaks (McPhaden et al., 2006). Droughts or floods leading to huge underproduction of various agricultural crops can have major economic impact (increased food prices), possibly leading to malnutrition and subsequent famine in poorer regions (McPhaden et al., 2006). Food security can potentially be improved both regionally and globally if deeper understanding of the ENSO impact on major crop production areas allowed for more advanced planning (Anderson et al., 2017). The economic impact of ENSO can, on the other hand, also be viewed as positive. US economy benefitted 20 billion dollars from a lower number of hurricanes striking the American coast under prevalence of El Niño conditions in 1997/98 (McPhaden et al., 2006). The fact that frequency of occurrence of both extreme El Niños and La Niñas is projected to increase under greenhouse warming (Cai et al., 2015a), globally causing more extreme weather events (regardless of their effect on the economy), further highlights the desire for more reliable and as precise as possible ENSO forecasts. Therefore, studies on topics like the one touched upon in this report are required.

In order to reach ENSO forecasts effectivity and its satisfactory precision in regions far from the Pacific which are affected by ENSO teleconnections, the ability to predict the timing of ENSO impacts is crucial. More recent publications assume a seasonal or two-months gap, ignoring possible strong month-to-month variability in ENSO impact (Philippon et al., 2014). This does not seem to be satisfactory and thus, this project aims to investigate the following:

1. Strength of the relationship between ENSO state and climate and vegetation anomalies in the selected regions in the study period 2001-2017.
2. Changes of these relationships with increasing time lag between the ENSO state and the climate and vegetation anomalies,
3. Differences of these changes for anomalies of temperature, precipitation and vegetation state and the different study areas.

Areas with an obvious ENSO impacts that have already been shown in other studies (summary maps are available as fig. 2 and 3 of this report) will be included in the analysis. As a result, distinct study areas to be tested will be located within the following regions: (a) Southern Africa, (b) NE South America, (c) Southern North America, (d) Indonesia, (e) SE Australia, (f) SE North America, (g) NW South America and (h) India. Global vegetation will be studied through satellite remote sensing.

The focus when analyzing the obtained results will be, among the main goal of studying the delay of ENSO impacts after its state, on the differences of this delay for climate and for vegetation anomalies, with the vegetation anomalies expected to be detected later (with longer delay) than the climate anomalies. Furthermore, it is expected that the time lag would vary for the different study regions, mainly with increasing distance from the ENSO forcing region in the equatorial Pacific.

2 Background

2.1 ENSO

El Niño-Southern Oscillation (ENSO) is one of the stable states of the Earth's atmosphere (Hannah, 2015) and has been one of the most frequent topics in scientific literature about inter-annual climate variability. Trenberth (1997a) cited Ropelewski and Halpert (1987) who claimed ENSO being the greatest source of climate variability on Earth after changing seasons, which is primarily caused by extraterrestrial factors, unlike ENSO. McPhaden et al. (2006), Philippon et al. (2014), Sterl et al. (2007) and Yeh et al. (2018) then perceived ENSO as the most important factor influencing Earth's climate year-to-year variability, with Anderson et al. (2017) adding the variability of crop yield on global scale. ENSO systematically impacts atmospheric circulation even in regions remote from its source area in the tropical Pacific through atmospheric changes driven by sea surface temperature (SST) alterations (Brands, 2017). Furthermore, Ahrens and Henson (2016) underlined that the whole Earth's average surface temperature may be increased by several tenths of a degree Celsius just because of an El Niño event: the strongest event of the instrumental record, El Niño 1997/98, contributed to 1998 being the warmest year of the 20th century, using average global temperature as a measure.

ENSO is featured by oscillation between two phases, a negative one called El Niño, and a positive one called La Niña. In fact, state of atmosphere and ocean in tropical Pacific, the area of ENSO occurrence, fluctuates between these two phases with an irregular period of 3–6 years (Trenberth, 1997b). McPhaden et al. (2006) mentioned a period of 2-7 years, Anderson et al. (2017) 3-7 years. Moreover, Roy et al. (2017) claimed that the frequency of different ENSO events might have changed in recent decades. This means that we often do not observe conditions derived from long-term averages, in which the opposite ENSO phases are smoothed into mean (ENSO-neutral) conditions (Trenberth, 1997b). According to Ahrens and Henson (2016), the tropical Pacific exhibits El Niño, La Niña and ENSO-neutral conditions

(neither of El Niño nor La Niña is in place) for approximately the same amount of time in the long-term.

Wang and Fiedler (2006) noted that the direct (and indivisible) link between El Niño as a purely oceanic and Southern oscillation as a purely atmospheric phenomena was first explained by Bjerknes in 1969. Since then, El Niño (in the ocean) and Southern oscillation (in the atmosphere) are considered manifestations of one complex phenomenon abbreviated as ENSO. Trenberth (1997a) further explained that for the oceanic state, El Niño only refers to the negative (or warm) phase as described above, not the whole oceanic component of ENSO phenomena. Conclusively, ENSO events cause changes not only in atmospheric, but also in oceanic circulation (Hannah, 2015).

Briefly described, ENSO event means occurrence of anomalously warm (El Niño) or cold (La Niña) conditions (Cai et al., 2015a). Anderson et al. (2017) defined ENSO as a coupling between anomalies in the atmosphere and equatorial Pacific Ocean. The so called Bjerknes feedback is ENSO's crucial feature (Anderson et al., 2017), depicting the coupling between the atmosphere and the ocean: temperature gradient between typically warmer western tropical Pacific and colder eastern tropical Pacific sea surface temperature (SST) is strengthened by increased intensity of equator-ward trade winds and vice versa (McPhaden et al., 2006). Upwelling of cool, nutrient-rich water to the surface off the South American coast, occurring during ENSO-neutral conditions when the trade winds necessarily lift the thermocline there, is limited with lower trade winds intensity (Yeh et al., 2018). This, simultaneously with the transport of warm surface water through the pacific countercurrent to the east along the equator, results in the warm SST anomalies during an El Niño event, reaching up to three degrees (Sterl et al., 2007) and consequent changes in spatial patterns of sea level pressure (SLP), leading to abundant rainfall and storms over the eastern Pacific (Ahrens and Henson, 2016). On the other hand, a La Niña event is caused by strengthening of the prevailing trade winds reinforced by the SST gradient between western and eastern tropical Pacific (Cai et al., 2015a), leading to larger than usual upwelling off tropical South America (Yeh et al., 2018), unusually strong westward transport of water vapor fueling deep convection (Anderson et al., 2017), lower-than-usual SLP values and excessive rainfall over the western Pacific (Ahrens and Henson, 2016). This whole cycle of trade winds and ocean water motions is called Walker circulation (Brands, 2017). An ENSO event typically lasts 1 – 2 years, develops in late northern hemisphere spring (Anderson et al., 2017) or summer (McPhaden et al., 2006) and its peak, observed as the time of the highest SST anomalies, is usually centered around the end of a calendar year, i.e. in northern hemisphere winter. Abdi et al. (2016) and Philippon et al. (2014) summarized it differently, stating that an ENSO event onsets in July, peaks in the following December-February, offsets in March-April and decays in May-June.

As McPhaden et al. (2006) noted, the same physical mechanism of spreading warm SST anomalies across the tropical Pacific during an El Niño event actually contributes to its offset as well. The anomalies propagate from the west to the east through waves in the surface layer of the ocean. These waves originate in the waters of the warm western Pacific and reflect back

westwards when reaching the eastern limit of the Pacific basin. This helps to reestablish the upwelling off the eastern Pacific coast and, through the Bjerknes feedback, the trade winds as well. If this mechanism is strong enough, the offset of El Niño is simultaneously an onset of La Niña. Conclusively, La Niña often follows El Niño, but typically not vice versa, and El Niño usually only persists one year, whereas La Niña can persist up to three years (Ahrens and Henson, 2016). In response to warming induced by increasing concentrations of greenhouse gases in the atmosphere, Cai et al. (2015b) found this mechanism to strengthen as they modeled 75 % of extreme La Niñas to follow directly (a year after) an extreme El Niño. Furthermore, they underlined the importance of the mechanism for keeping a balance between El Niño, La Niña and ENSO-neutral conditions since Walker circulation is expected to weaken with global warming. This would favor occurrence of El Niños only, if their offset did not inherently trigger a La Niña initiation. Anderson et al. (2017) even stated that all La Niña events occur exclusively after an El Niño, but only every second El Niño leads to development of La Niña.

Strong ENSO events alter not just the state of the atmosphere, but also the ocean – for instance, extreme El Niños turn easterly upper sea currents in the tropical Pacific into westerly (Cai et al., 2015a) and even parts of other ocean basins exhibit SST anomalies during ENSO events ((Roy et al., 2017) and Yeh et al. (2018)).

There has not yet been an agreement about what the physical cause of ENSO is (Cai et al., 2015a). Wang and Fiedler (2006) summarized theories about what causes ENSO as such into two groups: it is either a naturally occurring oscillation of both the ocean and the atmosphere which is self-sustained, or a mode triggered by a stochastic forcing, random in its nature. For the first option, four possible oscillatory models were proposed, with a fifth one uniting them (Wang and Fiedler, 2006). In terms of the stochastic forcing that could be responsible for ENSO, variation of tropical Pacific weather is mentioned the most often. It was, on the other hand, excluded that the Coriolis effect would be responsible for ENSO because of the equatorial location of ENSO forcing area (Wang and Fiedler, 2006).

2.1.1 Asymmetry between El Niño and La Niña and the two types of El Niño

In contrast to what was thought in 20th century, El Niño and La Niña should not be treated as exact opposites (Ahrens and Henson, 2016). Firstly, El Niños tend to be stronger than La Niñas (McPhaden et al., 2006). Secondly, not only the impacts, but even the processes leading to the two phases are asymmetric as the atmosphere tends to respond more to El Niño than to La Niña. This is caused by larger alteration of the pattern of convective heating over the tropical Pacific during the former compared to the latter (McPhaden et al., 2006). Cai et al. (2015a) justified it by greater influence of warm SST anomalies on zonal winds compared to the cold anomalies. The asymmetry is obvious in spatial patterns, duration, and how the events evolve in time (Roy et al., 2017). Furthermore, there are two types of El Niño events differing in the location of their SST anomaly centers within the equatorial Pacific, which is specified in their names: the Eastern Pacific (EP) or canonical El Niño and the Center Pacific (CP) El Niño, also referred to as El Niño Modoki (Roy et al., 2017). Fig. 1 depicts the spatial difference between the two types of El Niño events in terms of SST anomalies and the

definitions of regions used to calculate the anomalies. Takahashi (2015) concludes that an El Niño event is typically a combination of the two patterns evident in fig. 1.Roy et al. (2017) and Song et al. (2017) also suggest two analogical (CP and EP) types of La Niña. Fig. 2 shows the spatial difference between the two types of La Niña events analogically to fig. 1.

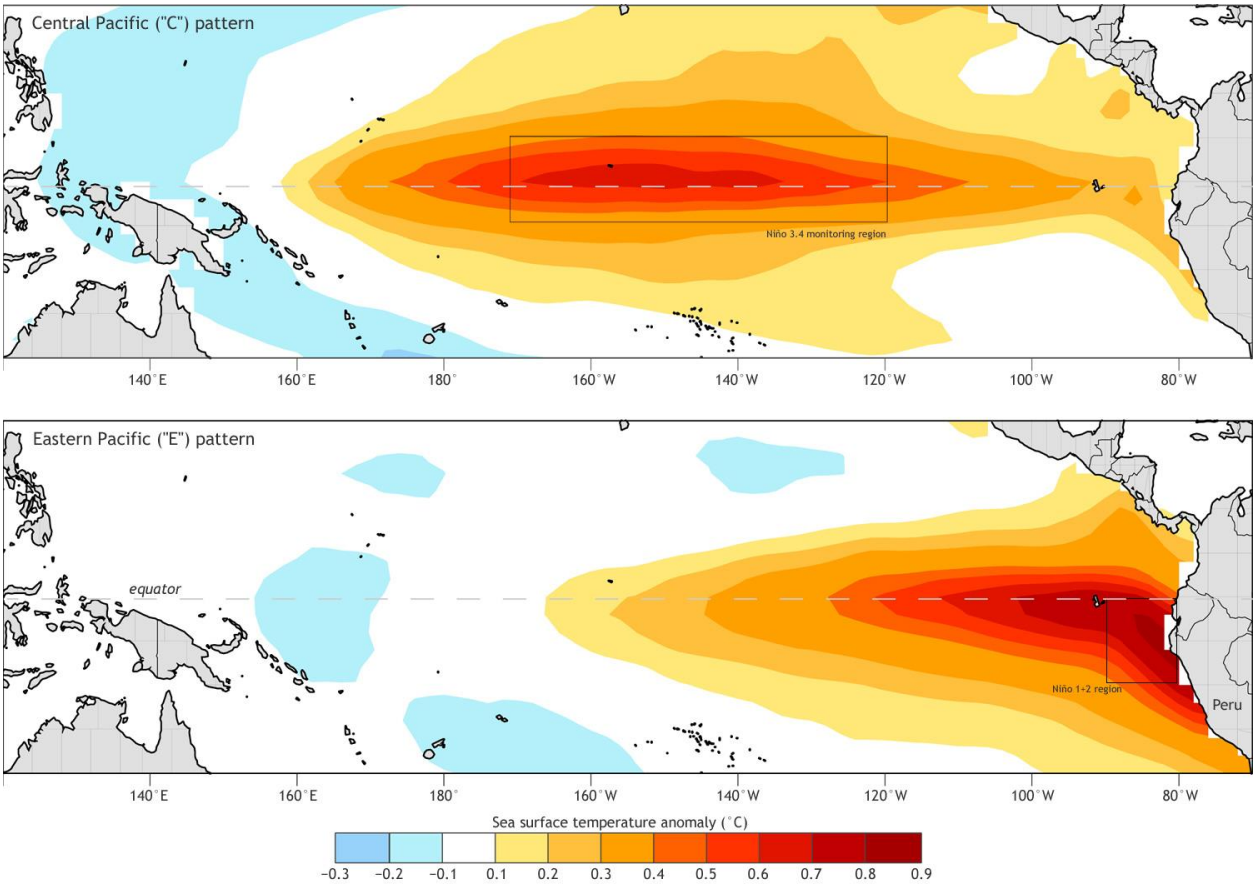

Fig. 1 – Comparison of spatial patterns typical for CP El Niño (upper panel) and EP El Niño (lower panel). SST anomalies are given in colors. Frames indicate the regions of the most pronounced anomalies during these two types of ENSO events, i.e. Nino3.4 region (upper panel) and Nino 1+2 region (lower panel). These regions are often used for calculation of SST anomalies defining the events. Source: Takahashi (2015). *Image courtesy of Ken Takahashi, reproduced with his permission.*

Moderate ENSO events differ in their dynamics from extreme ones even when comparing events of the same phase, introducing another degree of non-uniformity among ENSO events (Cai et al., 2015a). The SST anomaly center during extreme El Niños lies in the east of equatorial Pacific, but in its central part during both weak El Niños and extreme La Niñas, with weak La Niñas centering the anomalies in between the two aforementioned centers (Cai et al., 2015a). In fact, it seems that for El Niño events, the SST anomaly center moves eastward with increasing strength of the event (Cai et al., 2015a).

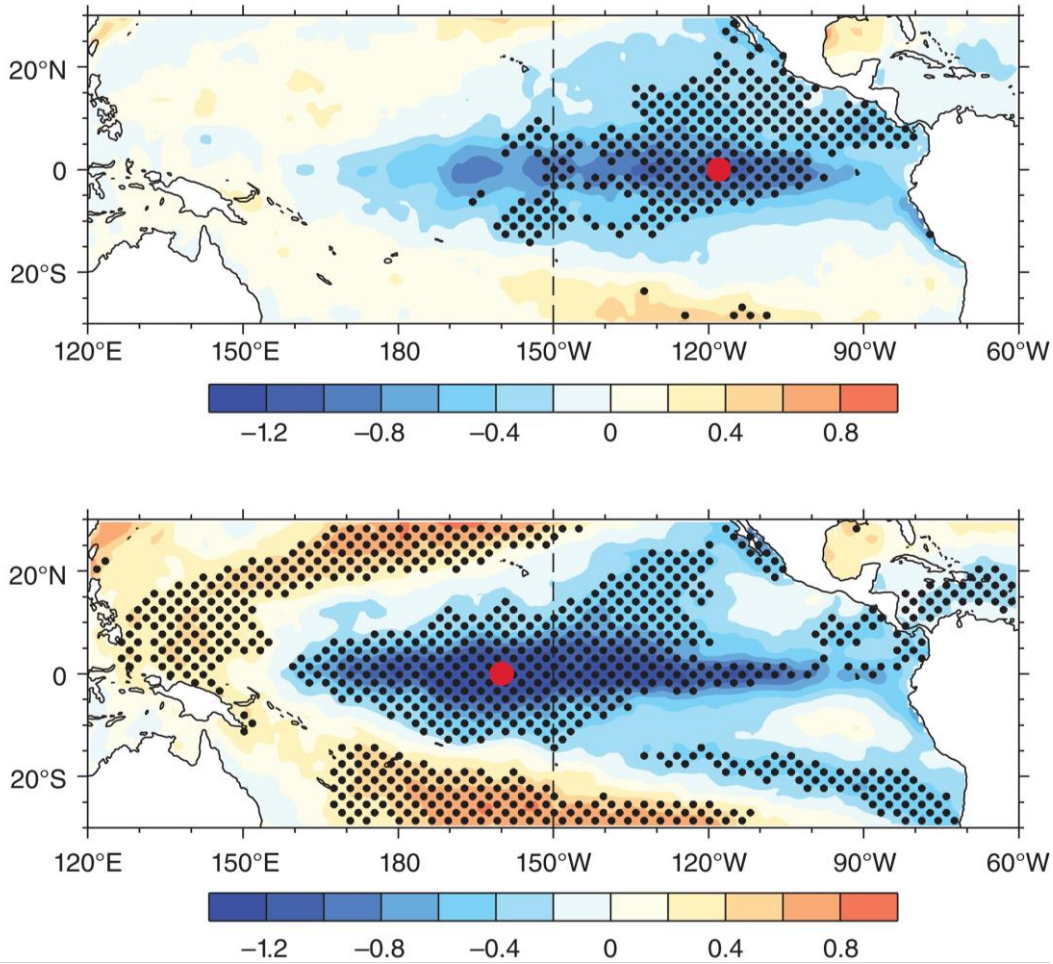

Fig. 2 – Composite of SST anomalies (°C) in the tropical Pacific during DJF for EP La Niña (upper panel) and CP La Niña (lower panel). The SST anomalies that are significant at the 90% confidence level are stippled with black dots. The red circles mark the locations of the maximum SST anomalies. Source: Song et al. (2017). *Image used with permission of Shangfeng Chen.*

2.1.2 Oceanic Niño Index (ONI)

In recent studies, Oceanic Niño Index (ONI), alternatively indices calculated similarly, seem to be the most common way of defining ENSO phases (Wolter and Timlin, 2011). It is described by e.g. Abdi et al. (2016): if a three-month running SST mean in Nino3.4 region (170 E – 120 W, 5 S – 5 N, marked in the upper panel of fig. 1) extends beyond an anomaly threshold of 0.5° C for at least five consecutive months, El Niño event is defined in case of a positive and La Niña event in case of a negative anomaly. Sterl et al. (2007) then defined Nino3.4 Index as the SST anomaly averaged over the Nino3.4 region itself. The base period used to calculate the anomalies is the most recently defined centered base period used by National Oceanic Administration (NOAA) National Weather Center (NWS) Climate Prediction Center (CPC), i.e. 1986-2015. The centered base periods were defined in order to define ENSO events by contemporary climatology of equatorial Pacific SSTs (Climate.gov 2016).

Trenberth (1997a) underlined that there is no universal definition of ENSO. Indeed, multiple indexes are available for ENSO depiction. As section 2.1.1 says, areas of SST anomalies occurrence vary among ENSO events. Thus, multiple areas for SST measurements from which indexes analogical to ONI can be used. Consequently, NOAA's CPC, from which the ONI index were obtained for this project, offers not just ONI and Nino3.4 Index as defined by Sterl et al. (2007), but also SST anomalies in areas with various spatial boundaries, named as Nino 1+2 (visible also in the lower panel of fig. 1), Nino 3 and Nino 4 regions.

Although virtually all studies cited in this report use the SST approach and mention it as the most effective and accurate way of defining ENSO, other approaches are also possible. Wolter and Timlin (2011) defined *MEI.ext* (where MEI stands for Multivariate ENSO Index), a more sophisticated index combining both SST and SLP (sea level pressure) values. Moreover, MEI.ext is not spatially constrained to fixed boundaries as these can be chosen individually for every study. Wolter and Timlin (2011) believe this to be the biggest advantage of the index, compared to ONI. On the other hand, ONI is significantly more appropriate of defining ENSO than Southern Oscillation Index (SOI), a traditional ENSO definition in the 20th century (Trenberth, 1997a). SOI was constructed as an anomaly of normalized difference between SLP values in Tahiti and Darwin (Tasmania).

Trenberth (1997a) warned that different ways of defining ENSO state could affect the results of any study where ENSO is involved.

2.2 ENSO Teleconnections

ENSO teleconnections can be described as atmospheric links between tropical Pacific and distant regions that result in climate anomalies (typically in precipitation and/or temperature) in the respective areas (Hannah, 2015). The mechanism of ENSO signal transmission is likened to gyres: one altered circulation cell projects the signal to the neighboring ones and thus affecting climate on long distances (Hannah, 2015). Abdi et al. (2016) depicted ENSO as the largest ocean-atmosphere teleconnection operating on large scales, while Brands (2017) perceived ENSO teleconnections as interconnected climate anomalies occurring in areas remote from each other. Ahrens and Henson (2016) defined teleconnections more specifically as SST anomalies' ability to influence precipitation patterns in distant regions of the Earth. Cai et al. (2015a) and Yeh et al. (2018) noticed the crucial role of teleconnections in affecting extreme climate events worldwide and weather patterns on planetary scale, Philippon et al. (2014) mentioned them as the way ENSO executes its global effect through various anomalies on various climate variables and Plisnier et al. (2000) pictured them as non-evidently linked weather anomalies occurring far away from each other.

Another definition by Cai et al. (2015a), quantitatively more specific, suggested that ENSO teleconnections are variations of values of a variable located far from the Pacific that are statistically significant and in line with ENSO variability. Possibly the most concise (and also touching the topic of this study) is the definition provided by Yeh et al. (2018), delineating teleconnections as statistically significant remote impact of the forcing region in the Pacific

occurring either simultaneously with underlying ENSO forcing or with a time lag. Ahrens and Henson (2016) then mentioned that the changes in atmospheric circulation caused by altered SLP as a result of SST anomalies propagate through rearrangement of the locations of dominantly rising or sinking air (i.e. SLP field).

Atmospheric convection over the region of warm SST anomalies, moved to the east during El Niño compared to ENSO-neutral conditions, is the starting point for extratropical El Niño-related teleconnections as it strengthens the regional Hadley circulation, resulting in enhanced subsidence in the subtropical part of the cell (Brands, 2017). In other words, the easterly move of rainfall and subsequent latent heat transfer triggers changes in the regional atmospheric circulation (McPhaden et al., 2006). Consequently, Rossby waves triggered by that anomalous heat source (Sterl et al., 2007) can transmit the ENSO signal to mid-latitudes (the so called Pacific North and Pacific South American patterns) within the system of subtropical anticyclones, whose circulation is affected by the anomalous subsidence in the subtropics as mentioned above by Brands (2017). It is also these wave trains that serve as the messenger of ENSO signal to extratropics and are thus responsible for ENSO teleconnections (Cai et al., 2015a). The mechanism for the spread of La Niña teleconnections is in principle analogic – enhanced Walker circulation over the western tropical Pacific weakens the strength of the regional Hadley cell including its subsiding motion in the sub-tropics, which again gives rise to anomalous features within the belt of sub-tropical anticyclones (Brands, 2017). It is also not irrelevant to mention that extreme El Niños move the Inter Tropical Convergence Zone (ITCZ) towards eastern tropical Pacific and the Southern Pacific Convergence Zone (SPCZ) one thousand kilometers northward, which itself disrupts usual weather patterns and causes weather anomalies (Cai et al., 2015a).

ENSO teleconnections affect both mean (seasonal) anomalies in the regions they impact as well as extreme events of the same sign, while the teleconnection mechanisms are the same in both cases (Yeh et al., 2018).

ENSO teleconnections also represent relevant input to global cycle of carbon, as reported by McPhaden et al. (2006). There are typically abrupt increases of global atmospheric CO_2 concentrations at the later stage of El Niño events, partly caused by alterations in the ratio between plants' respiration and photosynthetic uptake due to increased temperature, but mostly because of excessive tropical forest fires, triggered primarily by ENSO-driven droughts. The strongest recorded El Niño (in 1997/98) led to massive wildfires in Indonesia and thus undoubtedly contributed to the biggest annual increase of global atmospheric CO_2 concentration since the beginning of the records in 1957 until then (McPhaden et al., 2006). There is, however, typically a monthly to seasonal delay between the peak of an El Niño event and the abrupt rise in global atmospheric CO_2 concentrations, pointing to delayed vegetation response to El Niño teleconnections (McPhaden et al., 2006). Ahlström et al. (2015) considered ENSO the major source of interannual variability (IAV) in gross primary productivity (GPP) of semi-arid ecosystems that globally dominate both the IAV and the positive trend in land carbon sink.

2.2.1 Asymmetry between El Niño and La Niña and two types of El Niño

Different properties of different types of ENSO events as described in section 2.1.1 also lead to asymmetry in their teleconnections (Ahrens and Henson, 2016). In fact, the asymmetry in ENSO teleconnections is even bigger than that of SST anomalies of the underlying ENSO events (Cai et al., 2015a). Similarly, the two types of El Niño events, Eastern Pacific (EP) or canonical and Central Pacific (CP) or Modoki El Niño, produce different ENSO teleconnections because the location of the SST anomaly center that differs between these two is decisive for the development of ENSO teleconnections. Consequently, precipitation and/or temperature anomalies caused by EP El Niños tend to center more to the east of the affected regions compared to these caused by CP El Niños (Yeh et al., 2018). That, for instance, leads to findings such as the one of Ashok et al. (2007) which showed precipitation anomalies of opposite signs as a result of EP and CP El Niño over most of South America in northern hemisphere summer.

2.2.2 ENSO and its teleconnections and climate change

The validity of findings in ENSO teleconnections research may be underlined by the fact that there are no observed significant changes in their strength over the last century and only time scale extending over more than 100 years might reveal such changes (Sterl et al., 2007), implying that the record of ENSO teleconnections in past decades provides reasonable basis to draw conclusions about ENSO teleconnections in the coming decades. As a result, even if ENSO properties (its spatial extent, intensity etc.) alter under climate change, on which, according to McPhaden et al. (2006) and Yeh et al. (2018), there is no satisfactory agreement, the knowledge about ENSO teleconnections obtained so far can be superimposed on the altered ENSO patterns (Sterl et al., 2007). Moreover, a modeling study conducted by Cai et al. (2015b) showed that extreme La Niña teleconnection pattern on rainfall does not show any changes in the climate change period. Yeh et al. (2018) also showed that the eastern Pacific is one of only few ocean basins that has not been experiencing warming since 1990s, although it should in 21st century according to CMIP5 models.

ENSO activity was significantly stronger in 20th century compared to previous centuries, which Cai et al. (2015a) interpreted as empirical proof of ENSO "intensification" with greenhouse warming. Aside alterations of atmospheric circulation both in tropics and extratropics, general increase of tropospheric temperature due to inability of pressure gradients to persist during ENSO events contributes to propagation of ENSO teleconnections (Brands, 2017).

Nevertheless, Yeh et al. (2018) found the ocean mean state and hence also ENSO and ENSO teleconnections changed since 1990s: most importantly, the center of SST anomalies for both types of ENSO events shifted westwards in 1998-2015 in contrast to 1979-1997. Furthermore, the amplitude of El Niños seems weakened in the more recent of the two periods (roughly corresponding to the study period covered by this report), yet unchanged for La Niñas. However, the robustness of this change remains questionable (Yeh et al., 2018). And despite the fact that Cai et al. (2015a) did not see a major change in ENSO teleconnection patterns

with climate change, they predicted a general eastward shift of ENSO teleconnections as a result of an eastward shift of the underlying SST anomaly centers in tropical Pacific (Yeh et al., 2018).

Recently, there seems to be a general agreement on increased frequency of extreme ENSO events under climate change (Yeh et al., 2018). Moreover, higher El Niño frequency is expected to continue for up to 100 more years after the point at which the global mean temperature gets stabilized (Wang et al., 2017). Yeh et al. (2018) disagreed with the aforementioned statement by Sterl et al. (2007) and expected that also ENSO teleconnections would change with alterations of the mean state of climate and ENSO properties with progressing global warming, but admitted that there is no consensus yet on what specifically this change would be and that statistical significance of changes projected to certain regions is only marginal.

More studies which would shed the light on how ENSO and ENSO teleconnections change with climate change seem crucial since Yeh et al. (2018) showed that such changes are critical for occurrence and characteristics of extreme weather events. They also added that while there have been studies about ENSO impacts on anomalous mean values of climate variables, large uncertainties remained in confirming similar trends for ENSO effect on climate extremes. There is, however, base for optimism in terms of higher ability to model future ENSO behavior since approximately half of the fifth phase of the Coupled Model Inter-comparison Project (CMIP5) models were able to model ENSO realistically, which is a significant improvement from an older generation of models (CMIP3) and big steps forward also seem to be obvious in how models capture ENSO teleconnections (Roy et al., 2017).

2.2.3 Major ENSO teleconnections

The most typical examples of ENSO teleconnections include drought over Indonesia and Australia (McPhaden et al., 2006), weakening the Indian monsoon system during El Niño, drought over southern Africa and heavy rainfall in the western tropical South America and southern United States (Ahrens and Henson, 2016).

Forootan et al. (2016) confirmed that ENSO has an undeniable impact on Australian rainfall, although the Indian Ocean Dipole (IOD) can both strengthen and weaken the ENSO signal and the variability of Australian precipitation is hence the result of the influence of both ENSO and IOD. Their combined effect is particularly pronounced in southern hemisphere spring (September to November), the period of IOD peak and a developed ENSO event growing phase (Forootan et al., 2016). 43 % of non-seasonal precipitation variation was contributed to the combined effect of ENSO and IOD, with a time lag of one month (Forootan et al., 2016). In southern hemisphere winter (June to August), a positive IOD (exclusively) leads to limited precipitation over southern Australia and enhances the development of El Niño, while negative IOD being frequently accompanied by La Niña, creating way for impacts of its teleconnections in the region (Cai et al., 2011). Yeh et al. (2018) added that the Pacific Decadal Oscillation (PDO) has a huge effect on ENSO teleconnections to Australia,

typically weakening them in its positive phase, although its negative phase strengthens the effect of La Niña on Australian rainfall. Yeh et al. (2018) also emphasized significant seasonal discrepancies in anomalies caused by different types of ENSO events – the largest precipitation response to La Niñas (enhanced rainfall) and EP El Niño (suppressed rainfall, particularly in eastern Australia) occurs in southern hemisphere autumn (March to May), whereas the effect of CP El Niños is more apparent on limited southern hemisphere spring (September to November) precipitation in northern Australia. Whereas Roy et al. (2017) expected increased rainfall during La Niña as such, Song et al. (2017) added to the discrepancy between different impacts of different types of ENSO events, stating that precipitation anomalies over Australia are only pronounced during CP La Niña, not EP La Niña.

Particular is the ENSO impact on hurricane frequency and intensity: while El Niño leads to fewer and weaker Atlantic hurricanes and more Pacific hurricanes, La Niña has the opposite effect (Ahrens and Henson, 2016, McPhaden et al., 2006). Ahrens and Henson (2016) claimed that the likelihood of an Atlantic hurricane hitting the United States increases by 50 % during La Niña conditions compared to those of El Niño. McPhaden et al. (2006) mentioned three times higher likelihood during La Niña in contrast to El Niño. The "ENSO-extreme" period between 1997 and 1999, consisting of an extreme El Niño 1997/98 followed by an extreme La Niña, brought disastrous droughts to the western Pacific area in 1997/98, followed by severe floods just a year after (Cai et al., 2015b). At the same time, SW United States experienced reverse situation in that period – in fact, the 1998/99 La Niña-induced drought was one of the most severe on the record (Cai et al., 2015b).

Southern and SE North America experience wetter and cooler winters during an El Niño episode and, on the contrary, drier and warmer winters during a La Niña episode (Ahrens and Henson, 2016). Northern tropical Atlantic ocean SST typically increases after the peak of El Niño events in northern hemisphere spring (Yeh et al., 2018). A dipole pattern is created over North America in northern hemisphere winter and spring (December to May), expressed as opposite correlation values in response to ENSO forcing in Alaska and northern Canada on one side and Mexico and the US Gulf states on the other side (Brands, 2017).

According to Brands (2017), there was not any robust ENSO teleconnection to Florida in northern hemisphere summer and autumn (June to November). However, Anderson et al. (2017) found a clear precipitation anomaly in La Niña years, which took place concurrently with tropical Pacific SST anomalies and lead to both simultaneous, but mostly one season delayed correlation with soil moisture. There were also observed rainfall anomalies in winters of El Niño years, but interestingly, the stronger were the rainfall anomalies in El Niño years, the weaker were the anomalies in the following years which exhibited La Niña conditions (Anderson et al., 2017). Cold temperature extremes were observable in the region during El Niños, whereas anomalous frequency of warm extremes was typical for La Niñas (Yeh et al., 2018).

Indian summer monsoon precipitation is substantially limited during El Niños due to anomalous atmospheric subsidence over Indian Ocean basin caused by easterly shift of Walker circulation in the Pacific basin and the subsequent smaller contrast between SST and land surface temperature over the Indian subcontinent. La Niña has the opposite impact (Yeh et al., 2018).

Despite the fact that Brands (2017) did not find ENSO teleconnections to higher latitudes robust enough, there is excessive literature reporting on ENSO teleconnections on all continents, even including Antarctica (e.g. Turner (2004)). Fig. 3 summarizes El Niño teleconnections and fig. 4 La Niña teleconnections, both separately for northern hemisphere winter and northern hemisphere summer. ENSO teleconnections to other regions than the study areas covered by this report are, however, not further discussed here.

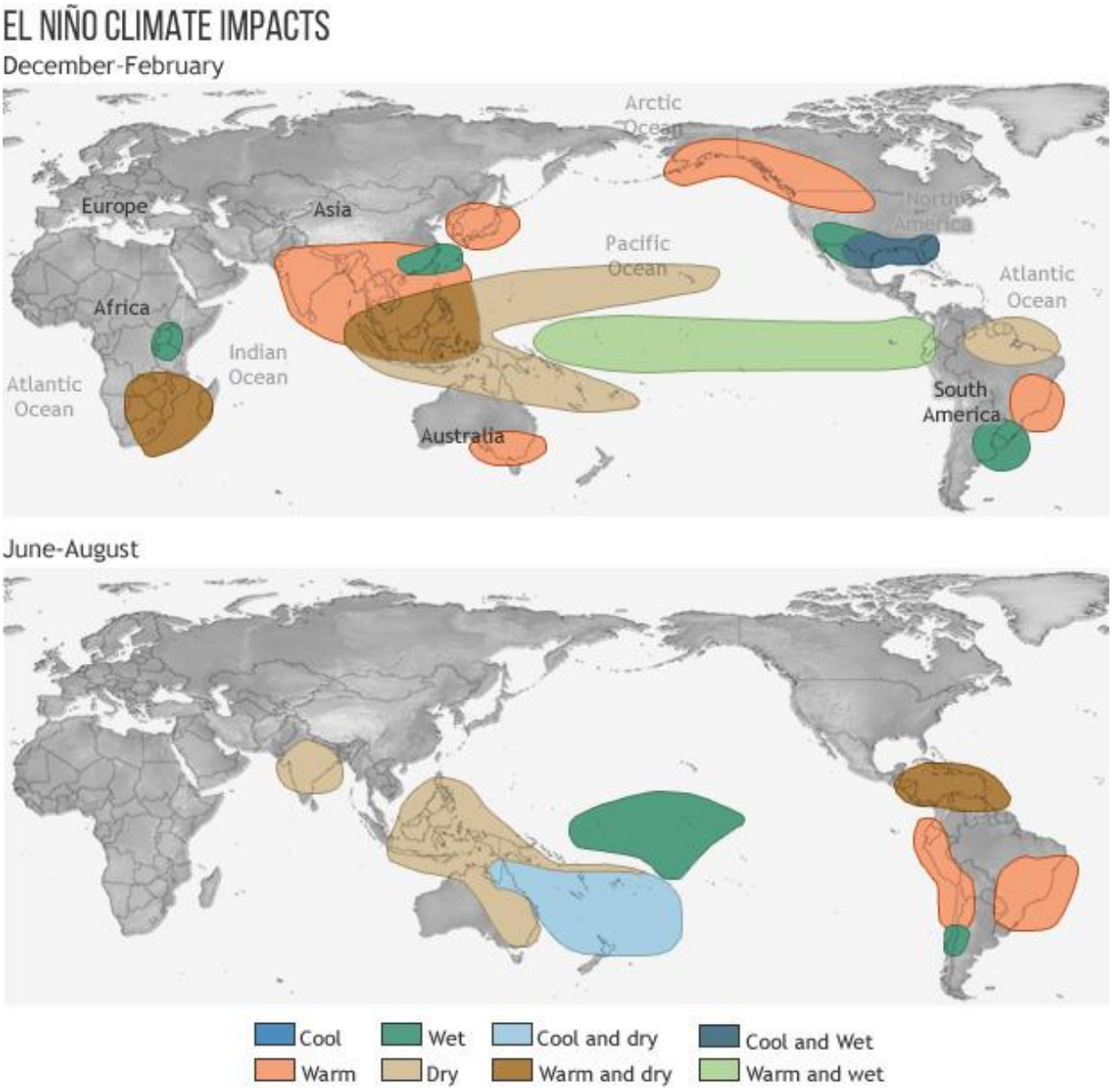

Fig. 3 – Typical El Niño teleconnections in northern hemisphere winter (upper panel) and northern hemisphere summer (lower panel). *Source: Climate.gov (2016).*

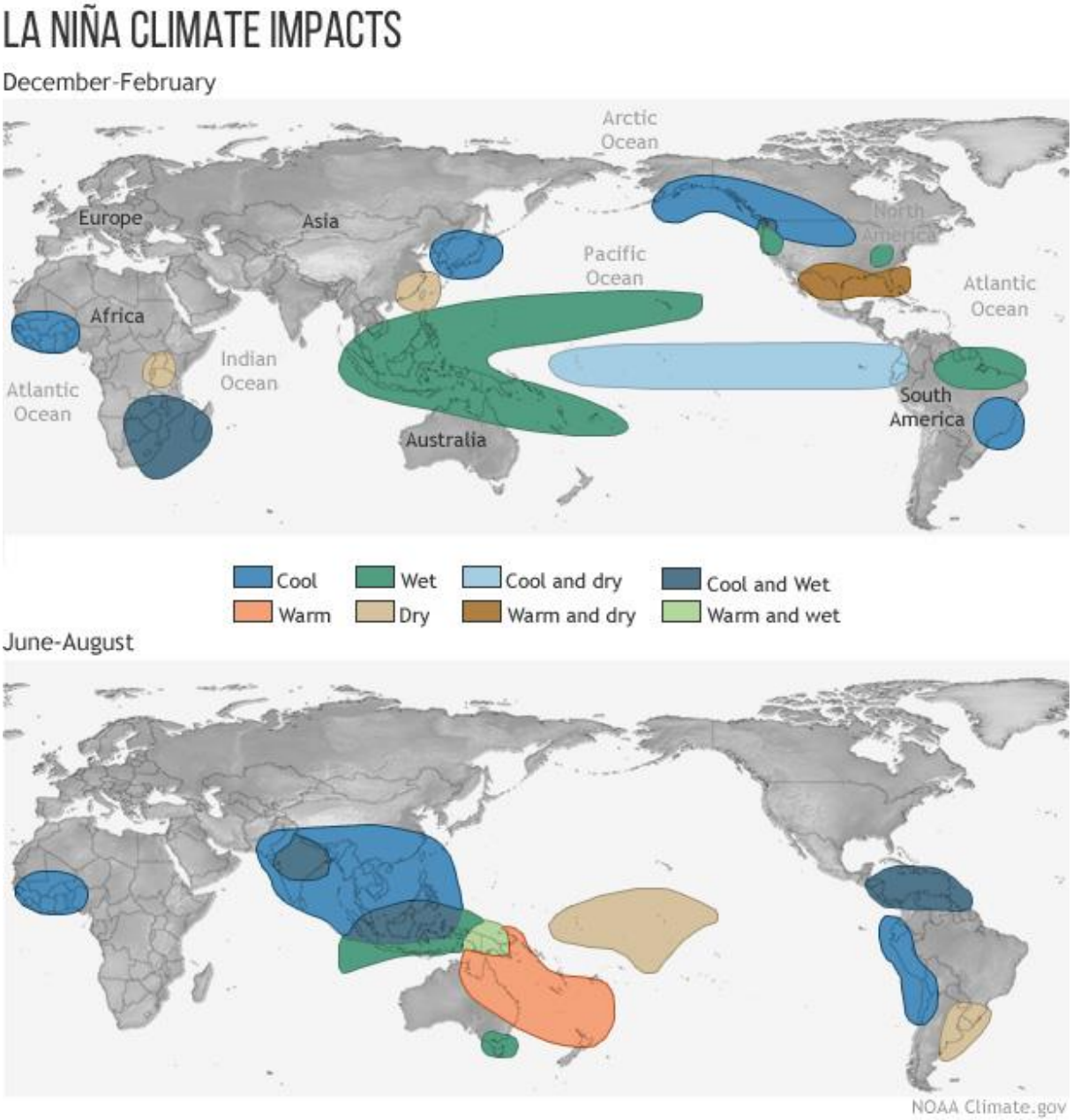

Fig. 4 – Typical La Niña teleconnections in northern hemisphere winter (upper panel) and northern hemisphere summer (lower panel). *Source: Climate.gov (2016).*

2.3 ENSO Forecasts

ENSO forecasts are now common and are used in policy-making and warning systems (Philippon et al., 2014) or relevant risk management strategies (McPhaden et al., 2006) and are, among others, of particular interest for agricultural sector (Anderson et al., 2017). McPhaden et al. (2006) claimed that ENSO is the most predictable feature of the climate system after changing seasons. Sterl et al. (2007) argued that the stationarity of ENSO teleconnections together with a rather long persistance of SST anomalies allow for research leading to seasonal and even annual forecasts. Ahrens and Henson (2016) underlined that while it is still very difficult to make a reliable ENSO prediction on a scale expanding few

months, it is more reasonable to issue a prediction for northern hemisphere winter conditions (the common peak phase of ENSO events) in northern hemisphere summer or autumn preceding the winter. The reason is that there usually already are sufficient signals to detect a coming ENSO event because SST anomalies established in northern hemisphere summer usually persist for at least two more seasons (McPhaden et al., 2006). This is why late spring of northern hemisphere was called a *predictability barrier* for ENSO forecasting, because after an ENSO event is developed (or not) in this typical time of an ENSO event evolution, the forecast for the next seasons could be pretty accurate (Trenberth, 1997a). Anderson et al. (2017) added that the strength of teleconnection is dependent on, although not exclusively, the magnitude of SST anomalies causing it.

On the contrary, Yeh et al. (2018) considered the predictability of ENSO teleconnections high only for Indonesia, eastern Southern hemisphereia and eastern Africa. Particularly for this paper, it is relevant to mention that the impacts of the strongest ENSO event covered by this report, the 2015/16 El Niño, were much weaker (apart from melting in West Antarctica) than these of precedent El Niños of similar strength in 1982/83 and 1997/98 (Yeh et al., 2018).

McPhaden et al. (2006) assured that successful forecast could progressively lower the economic losses caused by ENSO-sensitive phenomena. For instance, measures taken by governments, private sector and individuals in California in 1997/98 that followed a functional warning system report in response to a coming El Niño, summed up to saving one billion dollars (McPhaden et al., 2006). ENSO forecasting in the future is undoubtedly relevant as, despite uncertainties in modelling future ENSO behavior, there is an agreement on changes of the mean state and subsequent higher frequency of extreme ENSO events (Cai et al., 2015a).

2.4 Vegetation remote sensing and Normalized difference vegetation index (NDVI) in relation to this study

Satellite remote sensing is a tool of particular value when it comes to collecting information about the environment (Chuvieco, 2016). Studying the relation between climate and vegetation is one of the applications of satellite remote sensing (Jin and Eklundh, 2014). The satellites measure signals in different wavelengths, e.g. capturing different reflectance of different surfaces in different parts of the spectrum. In order to derive the amount of Earth's surface vegetation (greenness) from satellite imagery, vegetation indices (VIs), a robust and simple technique for this purpose, have been established (Chuvieco, 2016).

VIs utilize the fact that while green vegetation reflects only less than 10 % of radiation in the red (R) spectral region (wavelengths = 0.6-0.7 μm) in the visible part of the spectrum (VIS) because absorbs most of it, it reflects more than 50 % of the invisible near infrared (NIR) part of the spectrum due to significant leaf scattering. At the same time, soils and even brown vegetation have only marginal contrast in the reflectance in the two mentioned bands of the spectrum (Chuvieco, 2016).

Normalized difference vegetation index (NDVI) is one of the most common VIs used in vegetation remote sensing, profiting from its resistance towards non-vegetation noise and undoubtedly also the tradition of its use, resulting in availability of both spatially and temporally abundant data (Jin and Eklundh, 2014). Since it is a ratio index, it also minimizes other unwanted influences on the data such as illumination differences, cloud shadows or topographic variations (Chuvieco, 2016). It is calculated as following:

$$NDVI = (NIR-VIS)/(NIR+VIS),$$

where NIR stands for the surface reflectance in the near-infrared part of the spectrum and VIS for visible, alternatively red part of the spectrum as described above (e.g. Erasmi et al. (2014), Chuvieco (2016) or Philippon et al. (2014)). NDVI has a dynamic range from -1 to +1, with functional range for vegetation being 0 to 1 (Chuvieco, 2016).

The NDVI data acquired for this project originate from the Terra platform that is part of the NASA Earth-Observing System (EOS) program, particularly from the platform's main sensor, the Moderate-Resolution Imaging Spectroradiometer (MODIS). Terra was launched in December 1999. In the red and NIR spectral wavelengths used for vegetation monitoring, MODIS has spatial resolution of 250 m and daily observational frequency (Chuvieco, 2016). The particular MODIS product used in this project is described in the methodology section together with the other datasets used.

Plisnier et al. (2000) and Philippon et al. (2014) argued that in regions with poor coverage of meteorological stations providing validated climate datasets, vegetation indices, tested on large amount of studies, are the best way to capture ENSO teleconnections due to the data reliability and dense spatio-temporal coverage. Since the impact on vegetation and agriculture is often the most typical application of ENSO teleconnections studies (e.g. Anderson et al. (2017)), relating NDVI to ENSO seems more than meaningful. The following sections describe how temperature, precipitation and vegetation in the selected study areas were linked to ENSO state which was described above.

3 Methodology

The relationship between ENSO state and climate and vegetation anomalies was analyzed by correlating an ENSO indicator with a surface climate variable (temperature or precipitation) and a vegetation index (NDVI) respectively. The ONI Index based on tropical Pacific SST anomalies was used as ENSO indicator (available from NOAA Climate Prediction Center). Climate variables were acquired through a gridded (0.5° x 0.5°) dataset provided by University of East Anglia Climate research unit. NDVI data were obtained via the NASA LP DAAC website in the form of a gridded monthly dataset (0.05° x 0.05°). A more detailed description is given in section 3.2.

The inputs for the correlation analysis were the Nino 3.4 SST Index on the ENSO side and anomalies of monthly temperature, precipitation and NDVI values on the climate/vegetation side. The anomalies were calculated from the average of the time series used, which is 2001 to 2017. The Pearson correlation coefficient was used as a metric in the analysis. Again, more detailed information is in section 3.2.

3.1 Study areas selection

Parts of continents within which the study areas (a) – (h) are located are listed in the introduction. From now on, the regions are referred to with more specific names corresponding to their actual location. In table 1, they are listed in the same order (a) – (h) with the new names and defined spatially by their limiting coordinates.

Table 1 – Spatial limitation of selected study areas. Bordering latitudes and longitudes are given in degrees. The last column specifies the MODIS tile in which the NDVI data used in this study are stored for the respective study area.

Study area	*Lat S*	*Lat N*	*Lon W*	*Lon E*	*MODIS tile horizontal/vertical*
Africa	-28,5	-22,5	24,5	31,5	20/11
Brazil	-10	-5	-40,5	-35	14/9
Gulf of Mexico	22	30	-103,5	-95,5	9/6
Borneo	-4	0	110	117,5	29/9
Australia	-38	-30	147	153	30/12
Florida	25	30	-83	-80	10/6
Colombia	0	8	-77,5	-74	10/8
India	20	24	76	86	25/6

Maps of the study areas are available as fig. A1-A8 in the appendix.

The eight selected study areas were described and considered vulnerable to ENSO teleconnections by numerous studies, with some of them used as references in this discussion – e.g. Abdi et al. (2016), Anderson et al. (2017), Cirino et al. (2015). As a result, it was assumed that ENSO teleconnections would be evident in the climate and vegetation time-series in this study for at least one season, and thus that those areas would be appropriate for testing the time lag between ENSO forcing and the underlying climate and vegetation anomalies, without the necessity to test the ENSO impact on these regions as such or its statistical significance.

Finally, definitions of the exact borders of the study areas were affected by the spatial extent of MODIS tiles in which the obtained NDVI data are organized and stored. Conclusively, every study area lies within spatial boundaries of just one MODIS tile. Availability of this data was also decisive for choosing 2001 – 2017 as the study period covered by this paper.

3.2 Data processing

3.2.1 Data description I – climate variables and ONI

Precipitation and near-surface temperature are referred to as climate variables from now on as the processing was the same for both of them. Monthly means gridded time-series at 0.5° resolution from Climatic Research Unit (CRU) TS (time-series) datasets were downloaded for the study areas defined above for the study period 2001-2017 (Harris et al., 2014). Both datasets were terrestrial, i.e. portions of the study areas covered by seas were not part of the analysis.

ONI (see section 2.1.1) was used as ENSO indicator. It represents anomalies derived from three-months running average of sea surface temperature (SST) in Niño 3.4 region, i.e. 5N–5S, 170-120W. The base period used to calculate the anomalies is the most recently defined centered base period used by National Oceanic Administration (NOAA) National Weather Center (NWS) Climate Prediction Center (CPC), i.e. 1986-2015. The centered base periods were defined in order to define ENSO events by contemporary climatology of equatorial Pacific SSTs. ONI time-series specific for the seasons defined as for the climate variables (MAM, JJA, SON, DJF) were then created for the study period 2001-2017.

3.2.2 Data description II – NDVI

NDVI data were downloaded from the "MOD13C2" Version 6 product of NASA MODIS/Terra satellite. This product provides vegetation indices monthly, globally, in grid 0.05° x 0.05° degrees. More specifically, the monthly product is a result of weighted averaging of available (cloud-free, obtained every 8 days) satellite imagery for the month and location given. This product was resampled to 0.5° x 0.5° resolution so that the same format of matrices with the same temporal as well as spatial resolution as for the climate variables was obtained. As for the climate variables, the dataset did not cover pixels representing seas.

3.2.3 Data analysis – common for climate variables, NDVI and ONI

For every field of the grid in all the study areas, monthly average values of the climate variables and NDVI were calculated for the study period. Anomaly values for individual months were then derived from the average monthly means for 2001-2017 for all the grid points, separately for seasons: March-May (MAM), June-August (JJA), September-November (SON) and December-February (DJF).

The constructed monthly anomaly time-series for all the seasons and every grid point and the seasonal ONI time-series were divided by their respective standard deviations. In other words, z-scores (Abdi et al. (2016) call them standardized anomalies) were calculated for the time-series used. The z-scores were computed for each individual month but using the standard deviation of the season into which the respective month falls (i.e. MAM, JJA, SON, DJF) because it was the seasonal time-series entering the correlations. Conclusively, time-series of 51 values representing the three-month long seasons during the 17-years long study period of this project were correlated, with a z-score of a climate variable or NDVI on one side and a z-score of ONI on the other side. As a result, one Pearson correlation coefficient value was

obtained for both of the climate variables and NDVI for every month of the study period in every grid cell, representing the strength of the concurrent ENSO teleconnection in the grid cell.

To account for lagged-teleconnections, the same procedure as above was applied but correlating the z-score time-series of climate variables and NDVI with a delay of 1 to 11 months compared to the ONI z-score value. The lag (including the "zero lag" representing the concurrent teleconnection) with the highest value of the correlation coefficient was then considered the strongest ENSO teleconnection impact.

Correlation analysis was repeatedly used as a method for depicting effects of teleconnections (Hurrell and Deser, 2009). McPhaden et al. (2006) linked strength of the teleconnection to the intensity of the ENSO event causing it, suggesting that a linear correlation is an appropriate method for depicting ENSO teleconnections. In another study exploring ENSO teleconnections, Brands (2017) used Pearson correlation coefficient – just like in this study – linking seasonal mean SST spatially averaged over Niño3.4 region as predictor and a gridded climate variable as predictand. In order to quantify teleconnections, correlation was used also by Roy et al. (2017).

4 Results

4.1 ENSO events 2001 – 2017

During the study period January 2001 – December 2017, four events fulfilled the criteria (described in section 2.6) to be defined as El Niño events and five as La Niña events (fig. 5).

ONI time-series in the study period (fig. 5) showed that most of the nine detected distinct ENSO events followed the typical evolution of such (as described in section 2.1), i.e. evolving in northern hemisphere summer (June-August) and diminishing in early northern hemisphere spring (February – April) of the following year. The exceptions are (i) the weak La Niña of 2017 that only lasted to December of that year (after evolving in August of the same year), (ii) the La Niña 2007-2008 that persisted for a whole year since July 2007 until June 2008 and (iii) the strongest event of the study period, the El Niño that is usually described as the El Niño 2015-16, although the event fulfills the El Niño definition already since November 2014, lasting until April 2016. In terms of how "common" all the events were in terms of their characteristics, the El Niño 2004-2005 can be considered a weak event, but all the other El Niños (2002-03, 2009-10 and 2014/15-16) seem to be quite typical examples of its kind, allowing assuming them to cause typical teleconnection patterns shown by fig. 3 and fig. 4. The same applied for La Niñas 2007-08, 2010-11 and 2011-12, while these of 2008-09 and 2016 were just short and weak, which could possibly have been limiting for the evolution of typical La Niña teleconnection patterns.

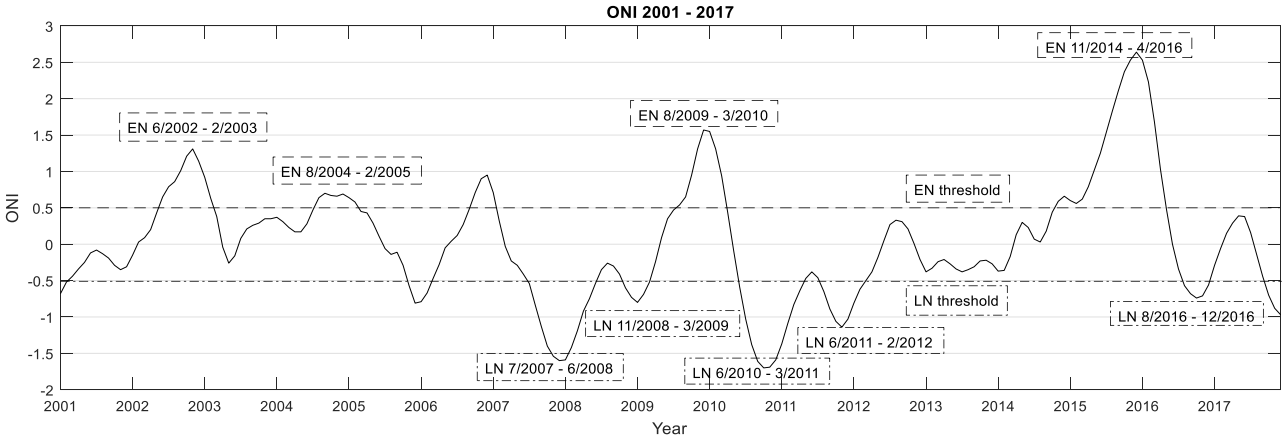

Fig. 5 – Time-series of ONI in the study period January 2001 – December 2017 with indicated thresholds that define El Niño and La Niña events (if reached for at least five consecutive months) and dated events fulfilling these criteria within the study period.

It would be abundant and too lengthy to show all the resulting matrices for all the study areas, variables, seasons and time lags. Instead, only a selection of all results considered relevant to address the aims of this project is mentioned here. Table 2 presents the main results regarding the time lag between ENSO state and ENSO teleconnections that were found strong enough. This was based on two criteria:

(i) The mean of correlation coefficients representing all the grid cells in a study area (area average) was higher than 0.3 or lower than -0.3.
(ii) There were at least four grid cells within a study area with correlation coefficient higher than 0.4 or lower than -0.4. The threshold of four grid cells was chosen because few matrices included one to three spatially isolated grid cells with values of the correlation coefficient exceeding the given threshold, but such correlation to individual grid cells were considered random since it was not accompanied by similar results in the neighboring grid cells.

If at least one of these criteria was fulfilled for a matrix of correlation coefficients for any of the examined variables in any of the study areas, the ENSO teleconnection was considered strong enough to use it for formulating the answers to the aims of this project. Yeh et al. (2018) noted that the observed correlations depicting ENSO teleconnections are relatively low due to considerable atmospheric background noise, suggesting that values stronger than 0.3 (a threshold set in the design of this study) indicate considerable teleconnection.

Table 2 – *Number of months of delay for which the value of correlation coefficient fulfills the set conditions (mean value for the whole study area >±0.3 or at least four grid cells within the study area with the value >±0.4) for all the variables (Prec, Temp and NDVI), seasons (DJF, MAM, JJA and SON) and regions tested. 51 pairs of values enter each individual correlation.*

	DJF		**MAM**		**JJA**		**SON**	
STUDY AREA	*Area mean >±0.3*	*Area max >±0.4*	*Area mean >±0.3*	*Area max >±0.4*	*Area mean >±0.3*	*Area max >±0.4*	*Area mean >±0.3*	*Area max >±0.4*
Africa								
Prec						10-11		
Temp					2	9		
NDVI						11		
Australia								
Prec						9-10		
Temp			11					
NDVI		3-4; 10						7
Borneo								
Prec		4						
Temp	4-5	4-5					5	
NDVI		8-9				10		6-7
Brazil								
Prec		9				9		
Temp			11		9			
NDVI				11				
Colombia								
Prec						10		
Temp		10				10		
NDVI		3; 10						6-8
Florida								
Prec								
Temp			8		10			
NDVI						4		6-7
Gulf								
Prec		4; 10						
Temp	5							
NDVI	4	3				4; 10		
India								
Prec		9-10				10		
Temp	4	4			10-11	10-11		
NDVI		4			10	10-11		6-7

4.2 Results organized by study area

4.2.1 Africa

Results showed positive correlation between JJA ONI values and April-July precipitation anomalies of the following year as well as with March-May temperature anomalies of the following year. This is in line with similar positive correlation with May-July NDVI anomalies of the following year. In other words, in years following an El Niño onset in JJA, southern Africa spatially defined as the study area *Africa* of this project experiences warmer, wetter and greener southern hemisphere autumn and winter, with La Niñas having the opposite effects.

There was also an evident negative correlation between JJA ONI and August-October temperature anomalies, leading to colder southern hemisphere springs during El Niños and warmer conditions during La Niñas. This result was very spatially coherent over the study area with negative correlation coefficient slightly below -0.3 present in almost all grid cells.

4.2.2 Australia

In terms of ENSO influence on rainfall, the only observed strong enough correlation between JJA ONI and 9 and 10-months delayed precipitation anomalies was constrained only to southeastern part of the study area. No other evident patterns were detected. The correlations with NDVI anomalies, suggesting ENSO influence on southern hemisphere autumn vegetation, showed contradictory tendencies – while the correlation was positive between SON ONI and southern hemisphere autumn NDVI anomalies, it was negative between DJF ONI and the same NDVI time-series. Thus, even if such ENSO forcing was present in the atmosphere, it might not be obvious in reality on the actual vegetation state in southern hemisphere autumn because the two opposite influences of ENSO would average out each other.

On the other hand, obvious negative correlation between DJF ONI and 10-months delayed NDVI anomalies indicated less green (greener) late southern hemisphere spring in SE Southern hemisphere following after El Niños (La Niñas), just with the exception of the south of the region. Finally, spatially very coherent correlation between MAM ONI and 11-months delayed temperature anomalies was detected over the whole region.

4.2.3 Borneo

Borneo, especially its southeastern part represented by the eastern half of the study area used here, showed a pretty strong negative correlation between DJF ONI and 4-months delayed precipitation anomalies, with values crossing -0.4 in the very east. At the same time, DJF ONI also exhibited a strong positive correlation with temperature anomalies present all over the island. This means exceptionally high April-to-July temperatures as a consequence of El Niños and anomalously cold conditions following La Niñas.

4.2.4 Brazil

NE Brazil experienced anomalously warm and dry MAM during El Niño and cold and wet during La Niña, respectively, due to 9-months delayed correlations with JJA ONI. Particularly obvious were these relationships by the Atlantic coast and in the southern and eastern portion of the defined study area, with especially the correlation with precipitation anomalies reaching almost -0.4 in the coastal region. Corresponding negative correlation was obtained for February-April NDVI response to MMA ONI of the preceding calendar year, i.e. less (more) greenness caused by El Niños (La Niñas), with the highest values of correlation coefficients again in the coastal part of the study area.

4.2.5 Colombia

Obvious positive correlation was found between JJA ONI and April-June rainfall anomaly (10 months delay), i.e. excessive (limited) precipitation followed El Niños (La Niñas). Values of the correlation coefficient were approximately uniform over the whole study area. Correlation of the same sign was observed also for temperature anomalies in the same period, especially in the southern portion of the study area, both in the coastal and inland region with the correlation coefficients over 0.4 in all grid cells.

4.2.6 Florida

Spatially very coherent positive correlation was detected between MAM ONI and 8-months delayed (November-to-January) temperature anomalies recorded over the whole Florida peninsula. Correlation of the same sign was observed between JJA ONI and 10-months delayed (April-to-June) temperature anomalies, a relationship stronger in the peninsular region than in the part neighboring with inland USA.

Correlations of the same sign were also found between ONI and NDVI anomalies, specifically between JJA ONI and 4-months delayed NDVI anomalies and SON ONI and 6-and-7-months delayed NDVI anomalies, resulting in NDVI anomalies basically concurrent with the temperature anomalies in October-to-December and March-to-June. It meant warmer and greener late northern hemisphere autumn and early winter following El Niño and vice versa following La Niña. However, the correlation coefficients were, unlike those expressing the correlation with temperature, higher in the inland portion of the study area than by the SE coast of Florida.

In contrast to all other study areas, no correlation that would fulfill the conditions set here was detected between ONI and rainfall anomalies.

4.2.7 Gulf of Mexico

Two evident positive correlations between DJF ONI and rainfall anomalies were detected: firstly, with delay of 4 months, and secondly, with delay of 10 months, mostly pronounced in the Mexican part of the study area by the coast. That meant wetter late northern hemisphere spring and late northern hemisphere autumn in El Niño years and, on the contrary, drier April-to-June and October-to-December following La Niña.

4.2.8 India

There were two seasons that experienced anomalies correlated with ENSO revealed by this study. The first one was late northern hemisphere spring and early summer. While no concise and strong enough correlation with precipitation anomalies was revealed, April-to-July temperature anomalies were correlated with both JJA as well as DJF ONI. All these correlations were positive, with the one between DJF ONI and 4-months delayed temperature somewhat weaker on the western edge of the study area, but with correlation coefficients mostly exceeding 0.4 in most of the area. The correlation between JJA ONI and 10-months delayed temperature anomalies exhibited the strongest correlation obtained for a climate variable in this project (in all study areas), with area mean of 0.41 and values exceeding 0.5 in northern part of the study area. Somewhat weaker, but still strong enough correlation (area mean = 0.33) with values between 0.3 and 0.4 everywhere apart from the NE corner of the study area was also detected for one month longer (11 months) delay.

Correlations for the same time periods were also evident for ENSO influence on NDVI, both with a negative sign. The correlation between JJA ONI and 10-months-delayed NDVI anomalies includes the strongest value of a correlation coefficient (-0.54) for any variable in any study area covered by this report. 11-month delayed correlation of the same kind as well as 4-months delayed correlation between DJF ONI and NDVI anomalies was also negative and evident enough, accompanying the aforementioned temperature anomalies, leading towards overall warmer (colder) and greener (less green) central India (corresponding to the study area India as defined for this project) in April-to-July following El Niño (La Niña).

Contradictory results were obtained for the correlation between SON ONI and 6-7-months delayed NDVI anomalies corresponding to March-June, roughly the same period as the one for which the ENSO influence were described in the two precedent paragraphs. Clearly positive correlation (with multiple grid cells experiencing correlation coefficient values higher then 0.4 up to 0.47) between ONI and NDVI anomalies was evident in the eastern half of the study area for the 6-month time lag and for basically the whole study area for the 7-month time lag.

Western half of the study area also experienced negative 9-10-month delayed correlation between DJF ONI and precipitation anomalies. This meant limited (excessive) rainfall in September-December after a peaking El Niño (La Niña) event the precedent northern hemisphere winter.

In order to demonstrate the outcome of the data processing before it was aggregated into the results presented in table 2, data for JJA ENSO teleconnections to the study region India are shown here in more detail. Fig. 6 plots mean, maximum and minimum values of the correlation coefficients obtained for the study region India against the time lag to ONI in months.

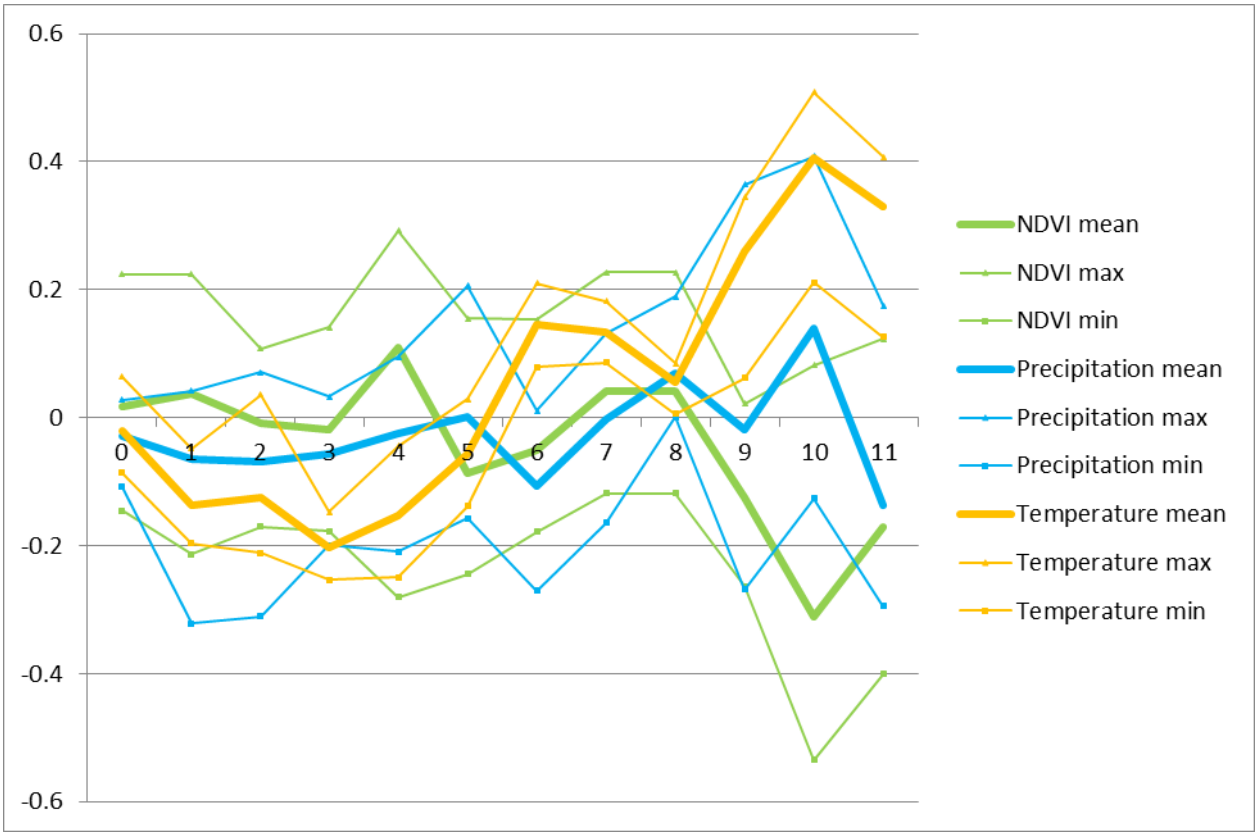

Fig. 6 – Mean, maximum and minimum values of the correlation coefficients for the three variables tested in JJA in study area India plotted against time lag to ONI in months.

Fig. 6 shows not only the largest correlation with the time lag of 10 months for all the three variables, but also the spread of values for every individual month being consistently the smallest for temperature, while bigger for precipitation and even bigger for NDVI.

Tables 3-5 show the obtained matrices of correlation coefficients for the 10-months delayed JJA correlations for the study region India (divided into grid cells 0.5° x 0.5 °). In order to easily glimpse over all the values in the study region, the matrices here are oriented west-to-east vertically (top-to-bottom) and north-to-south horizontally (left-to-right). This is because the general west-east orientation of the study area would not allow presenting all the values in one coherent table in a readable way.

The presented matrices present a generally spatially coherent ENSO teleconnection to temperature (table 5) with only little variation of values within one matrix, a result observable in most study areas. The correlation matrix for NDVI (table 3) shows higher variation of values, but the negative signal is still obvious in the whole study region. Table 4 then shows an example of a matrix depicting non-uniform result over the whole study area with a positive correlation centre in the southeast of the area (bottom right corner), but only weak correlation coefficients values in the whole western half (upper part of the matrix) of the study area. Nevertheless, variation between neighboring values is lower than for the NDVI matrix (table

3). More continuous matrices for precipitation than for NDVI were detected in most study areas.

	20N	*20.5N*	*21N*	*21.5N*	*22N*	*22.5N*	*23N*	*23.5N*
76E	-0.34	-0.08	-0.16	-0.08	-0.15	-0.30	-0.18	-0.36
76.5E	-0.41	-0.08	0.08	-0.12	-0.02	-0.15	-0.13	-0.40
77E	-0.37	-0.21	-0.25	-0.13	0.01	-0.11	-0.32	-0.42
77.5E	-0.35	-0.06	-0.33	-0.16	-0.06	-0.32	-0.25	-0.41
78E	-0.34	-0.23	-0.34	-0.25	-0.12	-0.37	-0.42	-0.54
78.5E	-0.35	-0.37	-0.39	-0.35	-0.20	-0.13	-0.07	-0.43
79E	-0.28	-0.41	-0.43	-0.34	-0.24	-0.28	-0.37	-0.42
79.5E	-0.11	-0.25	-0.41	-0.39	-0.16	-0.12	-0.42	-0.50
80E	-0.32	-0.13	-0.41	-0.44	-0.26	-0.18	-0.42	-0.45
80.5E	-0.25	-0.45	-0.43	-0.44	-0.46	-0.35	-0.45	-0.41
81E	-0.32	-0.47	-0.49	-0.53	-0.51	-0.17	-0.35	-0.40
81.5E	-0.28	-0.45	-0.47	-0.49	-0.23	-0.28	-0.43	-0.41
82E	-0.28	-0.49	-0.50	-0.47	-0.42	-0.42	-0.41	-0.32
82.5E	-0.40	-0.48	-0.38	-0.31	-0.36	-0.38	-0.33	-0.33
83E	-0.36	-0.41	-0.20	-0.30	-0.42	-0.37	-0.24	-0.13
83.5E	-0.40	-0.16	-0.24	-0.29	-0.49	-0.25	-0.19	-0.05
84E	-0.27	-0.28	-0.30	-0.39	-0.40	-0.33	-0.15	-0.09
84.5E	-0.22	-0.40	-0.35	-0.41	-0.35	-0.32	-0.27	-0.23
85E	-0.31	-0.31	-0.36	-0.37	-0.38	-0.31	-0.27	-0.27
85.5E	-0.29	-0.33	-0.40	-0.41	-0.37	-0.36	-0.38	-0.33

Table 3 – Matrix of the obtained correlation coefficients for NDVI for the 10-months delayed JJA ENSO teleconnection in the study region India. Note that the orientation of the matrices is west-to-east in the vertical direction (from the top to the bottom) and north-to-south in the horizontal direction (from the left to the right). Coordinates (in italics) are given for the northern, respectively eastern edge of the grid cells.

	20N	*20.5N*	*21N*	*21.5N*	*22N*	*22.5N*	*23N*	*23.5N*
76E	0.14	0.19	0.13	0.11	0.08	0.09	0.02	-0.10
76.5E	-0.01	0.13	0.12	0.10	0.10	0.09	0.05	-0.08
77E	0.10	0.12	0.11	0.10	0.09	0.08	0.00	-0.06
77.5E	0.16	0.17	0.10	0.10	0.10	0.05	-0.01	-0.09
78E	0.18	0.16	0.13	0.11	0.08	0.03	-0.04	-0.11
78.5E	0.16	0.15	0.14	0.11	0.07	0.01	-0.05	-0.11
79E	0.17	0.15	0.12	0.09	0.06	0.02	-0.07	-0.13
79.5E	0.17	0.13	0.11	0.08	0.06	0.03	-0.06	-0.11
80E	0.16	0.14	0.12	0.10	0.06	-0.01	-0.07	-0.11
80.5E	0.17	0.13	0.12	0.08	0.02	-0.04	-0.09	-0.11
81E	0.17	0.13	0.12	0.08	-0.01	-0.07	-0.10	-0.10
81.5E	0.19	0.17	0.15	0.09	-0.02	-0.09	-0.10	-0.10
82E	0.21	0.22	0.20	0.14	0.01	-0.06	-0.07	-0.07
82.5E	0.23	0.25	0.26	0.24	0.14	0.05	0.02	0.02
83E	0.23	0.26	0.30	0.32	0.29	0.20	0.13	0.11
83.5E	0.23	0.27	0.33	0.34	0.35	0.34	0.26	0.23
84E	0.24	0.29	0.33	0.36	0.37	0.36	0.35	0.32
84.5E	0.26	0.30	0.34	0.37	0.36	0.36	0.37	0.37
85E	0.26	0.30	0.34	0.36	0.37	0.37	0.38	0.39
85.5E	0.27	0.31	0.35	0.37	0.39	0.39	0.40	0.41

Table 4 – Matrix of the obtained correlation coefficients for precipitation for the 10-months delayed JJA ENSO teleconnection in the study region India. Note that the orientation of the matrices is west-to-east in the vertical direction (from the top to the bottom) and north-to-south in the horizontal direction (from the left to the right). Coordinates (in italics) are given for the northern, respectively eastern edge of the grid cells.

	20N	*20.5N*	*21N*	*21.5N*	*22N*	*22.5N*	*23N*	*23.5N*
76E	0.36	0.36	0.33	0.34	0.35	0.33	0.35	0.34
76.5E	0.42	0.42	0.43	0.34	0.34	0.31	0.33	0.33
77E	0.44	0.45	0.41	0.41	0.31	0.33	0.33	0.33
77.5E	0.43	0.44	0.42	0.42	0.32	0.31	0.31	0.31
78E	0.45	0.47	0.44	0.43	0.42	0.39	0.33	0.33
78.5E	0.45	0.46	0.46	0.45	0.44	0.41	0.33	0.32
79E	0.47	0.46	0.47	0.45	0.44	0.42	0.38	0.32
79.5E	0.48	0.45	0.47	0.46	0.43	0.40	0.38	0.37
80E	0.49	0.46	0.47	0.43	0.43	0.41	0.33	0.32
80.5E	0.50	0.45	0.45	0.43	0.42	0.43	0.41	0.35
81E	0.48	0.45	0.45	0.43	0.42	0.42	0.41	0.40
81.5E	0.48	0.49	0.46	0.43	0.43	0.42	0.41	0.40
82E	0.51	0.50	0.45	0.43	0.41	0.41	0.41	0.39
82.5E	0.48	0.51	0.46	0.44	0.43	0.42	0.41	0.40
83E	0.47	0.47	0.47	0.42	0.45	0.44	0.39	0.38
83.5E	0.43	0.42	0.44	0.42	0.43	0.40	0.37	0.37
84E	0.38	0.42	0.42	0.41	0.43	0.41	0.41	0.38
84.5E	0.41	0.40	0.44	0.41	0.42	0.38	0.40	0.39
85E	0.35	0.40	0.41	0.38	0.38	0.39	0.42	0.38
85.5E	0.21	0.26	0.27	0.35	0.42	0.37	0.33	0.38

Table 5 – Matrix of the obtained correlation coefficients for temperature for the 10-months delayed JJA ENSO teleconnection in the study region India. Note that the orientation of the matrices is west-to-east in the vertical direction (from the top to the bottom) and north-to-south in the horizontal direction (from the left to the right). Coordinates (in italics) are given for the northern, respectively eastern edge of the grid cells.

4.3 Common features of the obtained results for all study areas

Initially, when looking at for how many months of delay were the correlation coefficients peaking, almost all of them indicated the most detectable impact on the variables used in late northern hemisphere spring (roughly April to June). In other words, ENSO-caused anomalies seemed to be most evident in northern hemisphere spring and it was the delay of the ENSO teleconnections impact, not the season of occurrence of the ENSO event causing the teleconnections, what changed. As a result, typical observed delay for MAM ENSO teleconnections was 11 months (the longest tested in this study), 9-11 months for JJA ENSO teleconnections, 6-8 months for SON ENSO teleconnections and 3-5 for DJF ENSO teleconnections, where JJA and DJF teleconnections seemed to play major role in the overall ENSO teleconnections patterns, with evidently more frequent higher values of the correlation coefficients than SON and MAM teleconnections. It is very remarkable that none of the variables in none of the study regions indicated an evident ENSO teleconnection which would be simultaneous (equalling to delay of zero months).

Secondly, there was no obvious difference in the results for the climate variables and the vegetation state variable. This study did not clearly reveal any time gap between ENSO-driven precipitation and temperature anomalies and NDVI anomalies as these mostly appeared simultaneously in the results. On the other hand, the results obtained for SON teleconnections, where the set criteria for considering the teleconnection pronounced and included in the results of this study (specified and presented in table 2) were fulfilled in five

out of the eight study areas for the impact on NDVI (with the delay of 6-8 months), but for none of the areas for the impact on the climate variables.

Thirdly, there was hardly any obvious difference in the timing of ENSO teleconnections impact on different regions, despite their very varying distance from ENSO source area (the Nino3.4 region for this study). As specified in previous paragraphs, results of this study showed that it was the seasonal cycle which decided about the delay of the strongest ENSO teleconnections impact and this generally seemed universal for at least all the study areas covered by this paper, distributed over the tropics and subtropics. In other words, ENSO teleconnections impacted on the affected regions the strongest at basically the same time in northern hemisphere spring regardless of the location of the region.

Additionally, the obtained correlations also showed a tendency observable in all study areas: variability of values of the correlation coefficients within one resulting matrix (correlation between ONI and one of the variables for a specified monthly lag) is the biggest for NDVI, distinctly lower for precipitation and even lower for temperature. Nevertheless, in cases where a stronger correlation between ONI and NDVI anomalies was measured, the matrix of the correlation coefficients was relatively uniform as well (in terms of values), basically regardless of the study region (and a prevailing ecosystem).

Finally, there seemed to be a tendency in terms of the area impacted by ENSO teleconnections expressed with the values of correlation coefficients. These were not just more uniform, but usually also more widespread within the spatial extent of the study regions for temperature, less for precipitation and the least for NDVI.

5 Discussion

5.1 Prevailing time lags and spatial extent of the observed teleconnections

Most studies cited in this paper did not expect such long time lags suggested by the results of this study since they typically mentioned a delay of one season only. For instance, in their study *On the robustness of ENSO teleconnections*, Sterl et al. (2007) assumed that there is generally no need to account for a time lag in ENSO teleconnections at all, considering the short time the atmosphere needs to alter its state. Moreover, the method of correlating monthly averages inherently accommodates a time lag of couple of weeks anyway, although a lagged correlation might be relevant in some cases (Sterl et al., 2007).

Also Ahlström et al. (2015) expected the importance of accounting for lagged effect of climate drivers, namely precipitation, on the vegetation state, suggesting a semiannual time lag. However, this study did not show such pattern because there was no obvious difference in the time lag for different variables.

Regarding the impact of DJF teleconnections, it is important to keep in mind that the ONI time series might be temporally autocorrelated in times of an ENSO event evolution. Specifically, ONI values in northern hemisphere winter, at a typical peak of an ENSO event, are directly influenced by ONI values in the two preceding seasons during an onset phase of an ENSO event. Therefore, it might be considered wrong to draw a conclusion that, e.g. exclusively DJF ONI has an impact on climate/vegetation anomaly of the region even if it was the only season with a measured effect, because the DJF ONI would not exhibit the values it does without the trend in the two preceding seasons.

Brands (2017) also noticed the trend indicated by results of this paper that the spatial extent of the area of ENSO teleconnections-triggered temperature anomalies generally tends to be bigger than that of precipitation anomalies, at least in tropical regions.

5.2 Observed teleconnections to the study areas

Since the knowledge of mechanisms triggering ENSO is still on a rather hypothetical level, causes of ENSO and its teleconnections remained beyond the scope of this project and the report mostly stayed within descriptive level when it comes to discussing the observed results.

5.2.1 Africa

Philippon et al. (2014) calculated with two months lag between Nino3.4 index and NDVI in their study covering the whole of Africa, but with no time lag between Nino3.4 index and climate variables on a monthly scale, backing such approach with a positive correlation between precipitation and two months-lagged NDVI in their study area. This is not what the results of this study in southern Africa supported.

Abdi et al. (2016) reported drier than usual conditions during El Niño and typically wetter conditions during La Niña in most of southern Africa and assumed a positive correlation between an ENSO event and its impacts on the region, i.e. severe droughts caused by strong El Niños and floods in response to extreme La Niñas. Nevertheless, such a conclusion could not be made from the results of this study. It is possible that the precipitation extremes mentioned by Abdi et al. (2016) only follow extreme ENSO events, of which only one (El Niño 2015/16) was on the record spanning the period of this study.

The findings of Yeh et al. (2018) about warm and dry extremes detected during El Niños and cold and wet extremes during La Niñas in southern Africa were also not confirmed. Neither was the one about positive temperature anomaly in southern Africa in northern hemisphere summers preceding the northern hemisphere winter peak of CP El Niños (Yeh et al., 2018). On the contrary, there was a spatially very coherent negative correlation between JJA ONI and August-October temperature, indicating colder late northern hemisphere summers before the winter peak of El Niños and warmer in La Niña years. An explanation to such non-coherent results among studies can be that of Diaz et al. (2001) cited by Brands (2017), who proclaimed ENSO teleconnections to the southern hemisphere of Africa not robust enough,

allowing any possible results for correlation between ENSO state and the variables in question in southern Africa due to too much weather noise.

5.2.2 Australia

It may be the complex interplay of the different climate phenomena (ENSO, IOD, PDO – see section 2.2.3) what prevents this project getting similar results like those of authors mentioned in section 2.3.3. In terms of rainfall, the only big enough values of the correlation coefficient were detected between JJA ONI and March-June rainfall anomalies of the following year, which suggested a different result than the aforementioned studies: higher (lower) than usual rainfall values as an outcome of El Niño (La Niña). This result was, however, spatially very limited to southeastern part of the study area, the rest of the region did not show such pattern.

Yeh et al. (2018) claimed that ENSO also affects extreme weather over Australia: warm and dry extremes markedly occur during El Niño and cold and wet extremes during La Niña. Although, as mentioned above, the impact of ENSO on rainfall was not proved in this paper, the observed correlations between ONI and temperature and NDVI anomalies as described in 4.1.2 confirmed the tendencies provided by Yeh et al. (2018).

5.2.3 Borneo

Brands (2017) found ENSO being the major modulator of precipitation regime over the entire Indonesia. Looking at historical records, Keil et al. (2008) found that 93 % of all drought events over Indonesia between 1830 and 1953 were coupled to El Niño, with Yeh et al. (2018) confirming occurrence of extreme drought following El Niños also in recent decades. On the other hand, La Niña 1998/99 brought floods and land-falling tropical cyclones to the area (Cai et al., 2015a), confirming the statement of Yeh et al. (2018) that positive rainfall extremes generally occur in La Niña years. Furthermore, Yeh et al. (2018) found an ENSO teleconnection to South China Sea, bordering the west of the respective study area in this project, lagged by 3 – 6 months.

These findings were confirmed by the detection of negative correlation between DJF ONI and 4-months lagged precipitation anomalies. Moreover, extreme warm temperatures in SE Asia are concurrent with El Niño and extreme colds with La Niña (Yeh et al., 2018). This is fully supported by the findings of this study for April-to-July temperature anomalies caused by DJF ONI. Actually, the correlation between ENSO state and temperature anomalies over Borneo was even more evident than the correlation with the precipitation anomalies.

5.2.4 Brazil

Both Brands (2017) and Sterl et al. (2007) found ENSO teleconnections pronounced over the whole tropics, thus including NE South America. They found ENSO-related anomalies in NE South America corresponding to the study area called Brazil in this project in MAM. This goes hand in hand with the observed negative correlation between JJA ONI and 9-months delayed (i.e. MAM) precipitation anomalies and positive correlation with 9-months delayed (MMA) temperature anomalies. Cirino et al. (2015) found precipitation decrease and above

average temperatures in the region in response to El Niños and positive rainfall, but negative temperature anomaly caused by La Niña events. The sign of anomalies to the two types of ENSO events was the same in this study. Also Roy et al. (2017) confirmed deficient precipitation in equatorial South America following EP El Niño.

Anderson et al. (2017) found MAM vegetation anomalies in South America caused by the preceding DJF SST anomalies, whereas MAM SST anomalies were insignificant. According to them, the largest SST and precipitation anomalies occurred simultaneously without any delay and only weaker anomalies were accounted to lagged teleconnections. That was not proven by this study since the only NDVI anomaly fulfilling the consideration criteria set here was the one with MAM ONI delayed by 11 months, with three seasons longer delay than mentioned by Anderson et al. (2017). The authors themselves, however, offered a potential explanation for the disconnect in results of this and theirs study: in northern hemisphere spring (after ENSO events peaking), NE Brazil precipitation anomalies exhibit a typical case of different EP and CP El Niño teleconnections – the rainfall anomaly is negative for the former, but positive for the latter (Anderson et al. 2017). Correlations were not calculated separately for EP and CP El Niños in this project.

On the other hand, Erasmi et al. (2014) found the highest correlation between Nino3.4 index and precipitation with time lag of 10 months, with relatively high and similar values for time lags up to 11 months, but much lower values exceeding that lag. This is very close to findings of this study which detected the biggest correlation between ONI and precipitation anomalies at 9-months delays for DJF and JJA ONI. However, this project did not confirm similar values of the correlation coefficients for shorter delays, only for time lags of 8 to 11 months. Moreover, Erasmi et al. (2014) found the strongest correlation between Nino3.4 index and NDVI with time lag of 12 months, with an approximately linear increase of correlation values with longer time lag up to 10 months lag, slight increase up to the maximum at 12 months lag and an exponential, but initially not very steep decrease beyond that time horizon. This study revealed an evident negative correlation between MMA ONI and 11-months delayed NDVI anomalies, which is again close to results of Erasmi et al. (2014), but just like with precipitation anomalies, no similar results were obtained for the preceding months. Cirino et al. (2015) also observed ENSO teleconnections impact on maize and soybean yield: lower in El Niño years and higher in La Niña years, which is in line with the aforementioned NDVI anomalies and corresponds to the observed underlying precipitation and temperature anomalies.

5.2.5 Colombia

Anderson et al. (2017) reported strong precipitation anomaly in Colombia in northern hemisphere winters of La Niña years, with droughts recorded, for instance, from the 1998/99 event (Cai et al., 2015a). Results of this study, however, did not indicate any strong linear relationship between ENSO and rainfall anomalies in DJF.

On the other hand, Roy et al. (2017) found CP El Niño bringing anomalously excessive rainfall to the region. This was confirmed here for April to June precipitation anomalies caused by ONI in JJA of the preceding year. Given the varying topography of the study area (being divided by the Andes from north to south), values of the correlation coefficients were surprisingly uniform over the whole area. Such result could mean an advantage of the calculation method used, utilizing standardized anomalies as values correlated with the ENSO indicator. As a result, while the western slopes of the Andes had significantly higher mean monthly rainfall than the eastern portion of the study area, the detected standardized anomalies were much more similar on both sides of the Andes.

Yeh et al. (2018) reported on colder northern hemisphere summers caused by CP El Niños. Such finding was not supported by the results of this project. The only evident ENSO impact on temperature in the region revealed was a 10-months delayed positive JJA ONI correlation to rainfall, signalizing, on the contrary to Yeah et al. (2018), higher (lower) April-June temperatures following an El Niño (La Niña) event.

5.2.6 Florida

This study roughly confirmed the lack of ENSO impact in northern hemisphere summer and autumn found by Brands (2017), with the periods affected consisting of October-to-January and March-to-June in the results of this study. There was, however, no precipitation anomaly concurrent with tropical Pacific SSTs mentioned by Anderson et al. (2017). In fact, Florida was the only study area covered by this report in which there was not detected any strong enough correlation with precipitation anomalies that would fulfill the criteria set for the anomaly to be considered profound enough (see table 2). Reasons for such disagreement in results could potentially include a big role of Atlantic hurricanes affecting the precipitation records in the area, especially in La Niña years (Cai et al. 2015) to the extent that it disabled detection of a linear relationship between ENSO state and precipitation over Florida.

Neither could be the ENSO influence on temperature as described by Yeh et al. (2018) confirmed. On the contrary, the obtained results obtained pointed to warmer (colder) than usual conditions in November-to-January during El Niños (La Niñas) detected in MAM as well as in April-to-June, as a result of JJA ONI. Possible explanations for this contradictory result could be a somewhat different study design, with this paper presenting results using a method discovering linear relationships between ENSO and the selected variables, while Yeh et al. (2018) mention precipitation extremes typically occurring during certain ENSO conditions, which is something else than a consistent linear impact. Moreover, a very critical approach towards the result of ENSO conditions in MAM influencing precipitation in Florida regardless of the length of the time lag is more than appropriate specifically in this case as MAM is typically a season of ENSO neutral conditions (see fig. 9), with only the two longest events in the study period (La Niña 2007/08 and El Niño 2014(15)/16) in place during MAM.

5.2.7 Gulf of Mexico

While, according to Brands (2017), ENSO teleconnections did not seem to be sufficiently significant in northern hemisphere summer (JJA) and autumn (SON), positive correlation was observed between Nino3.4 SST and precipitation in Mexico and SW United States during northern hemisphere winter (DJF) and moreover, it was found robust to any internal atmospheric variability. Anderson et al. (2017) found a strong northern hemisphere winter precipitation anomalies over the region too as well as Yeh et al. (2018) during Central Pacific El Niños. Such findings were, however, not supported by the results of this study since no strong enough correlations were found for northern hemisphere winter.

In Mexico, Adams et al. (2003) found El Niño years warmer, yet wetter than La Niña years, but with a summer discrepancy to the observed annual trend, since El Niño typically meant below average precipitation and La Niña above average precipitation in the region in summer months. Anderson et al. (2017) observed maximum temperature anomalies in El Niño years. Results of this study confirmed positive temperature anomalies in May-to-July as well as negative rainfall anomalies in April-to-June as a response to DJF ONI, corresponding to what Adams et al. (2003) described as the summer discrepancy. However, the only other strong enough correlation was found between DJF ONI and October-to-December precipitation anomalies (10-months delay), and thus of the positive sign, really meaning wetter (cooler) conditions caused by El Niño (La Niña). Nevertheless, these positive correlations did not occur simultaneously, despite both being caused by DJF ONI. The northern hemisphere winter precipitation anomalies occurring simultaneously with tropical SST anomalies found by Anderson et al. (2017) were thus not detected by this study.

5.2.8 India

ENSO greatly modulates the Indian summer monsoon which in turn is principal for the nation's economy (mostly agriculture) since it is responsible for up to 80 % of mean annual rainfall (Roy et al., 2017). El Niños cause serious droughts over India with limiting Indian summer monsoon rainfall in northern hemisphere summer and early fall, i.e. before the ENSO events peak in northern hemisphere winter (Yeh et al., 2018). CP El Niños recently seemed to be more effective in suppressing the monsoon rainfall than EP El Niños, but the negative precipitation anomaly was obvious in both cases (Yeh et al., 2018). In the region corresponding to the study area covered in this report, precipitation was clearly suppressed in northern hemisphere summers by both EP and CP El Niño events and, on the contrary, enhanced by La Niña, although the magnitude of such impact seemed lower than that of El Niño (Roy et al., 2017). Nevertheless, this result was very obvious in the study area with the method used in this project for northern hemisphere summer, but instead for northern hemisphere autumn in the western portion of the study region. Results obtained by this study thus suggest the same impact, but its different timing.

On the other hand, Yeh et al. (2018) mentioned positive rainfall extremes typical for northern hemisphere winter of El Niño years, potentially to certain extent compensating for the

antecedent drought on annual scale, with the opposite pattern of extreme rainfall in La Niña years. However, such impact was not confirmed by the results of this study.

Anomalous temperatures in response to ENSO occurring in India were reported too – warm extremes during El Niño and cold during La Niña (Yeh et al., 2018). Brands (2017) revealed a distinct spatio-temporal pattern of the ENSO teleconnection strength, being the strongest in the north of the subcontinent in northern hemisphere summer (JJA), i.e. at the onset of the monsoon season, and gradually moving southward, reaching its highest intensity in the south of the subcontinent in northern hemisphere autumn (SON), i.e. at the end of the monsoon season. The area of altered rainfall was reported to be generally more spatially concentrated than the more extensive one of temperature (Brands, 2017). This project suggested similar comparison like the one above with rainfall anomaly – while the observed impact on temperature was confirmed as suggested by Yeh et al. (2018), its timing as described by Brands (2017) was not, because this study indicated the season of most pronounced anomaly in April-July.

Aside methodological reasons, a possible explanation for the discrepancies in results presented by this paper and the other studies cited here is the one presented by Roy et al. (2017): the correlation between ENSO and Indian summer monsoon is getting lower in recent decades (which corresponds to the study period covered by this paper). Underlying causes for it remain on a hypothetical rather than proven level (Roy et al. 2017).

5.3 Factors influencing results of this study

5.3.1 Correlation as a method and statistical handling of the data

Some of the discrepancies between results of this study and those presented by other authors could be explained by different methodology and/or data processing. Aside correlations, linear regression coefficient of the climate variable on Niño3.4 index can be used. This was done by Sterl et al. (2007) who correlated Niño3.4 index with anomalies of a climate variable to capture a teleconnection and used the linear regression coefficient to quantify its strength and accordingly proclaimed an ENSO event strong if the Niño3.4 index exceeded one standard deviation. Regression was also used as a method by, for example, Cirino et al. (2015). Abdi et al. (2016) used lagged ordinary least squares regression and Forootan et al. (2016) used multi linear regression (MLR) and also Hilbert transformation. For the sake of the lagged teleconnections analysis, Anderson et al. (2017) used partial correlation analysis to eliminate the effect of concurrent anomalies in order to only consider the previous season anomalies so that the observed anomaly is only the result of the time period in question in the lagged correlation analysis.

Different definitions of the base period from which the tropical Pacific SST anomalies were departed could also be a reason for non-coherent reasons among studies. For instance, Abdi et al. (2016) used 1971 – 2000 as the base period, but the ONI index used in this project calculates the anomalies from 1986 – 2015 averages.

The nature of values entering the correlation analysis is another topic worth a discussion. Rather than using raw values of the climate variables, Plisnier et al. (2000) recommended to calculate their Z-scores (also referred to as standardized anomalies by Abdi et al. (2016)) and correlate them with an ENSO index. This was also the approach used in this study. Erasmi et al. (2014) then suggested comparing the rankings of values instead of raw data (and using Mann-Kendall test for monotonic trends) in order to avoid unwanted influence of outliers on the result. Smoothing the anomalies over time was another common practice – for instance, Erasmi et al. (2014) and Philippon et al. (2014) used three-month running window, while Plisnier et al. (2000) expanded the running window to five months. Calculation of ONI index used in this project includes three-month running window for calculation of SST anomalies.

Furthermore, different approaches to vegetation indices are possible – Plisnier et al. (2000) and Erasmi et al. (2014) used maximum value composites (MVC), accommodating the highest value derived from a merge of two bi-monthly images for each pixel. Abdi et al. (2016) used the same approach for net primary productivity (NPP) values (not a vegetation index) in a study with otherwise similar design. On the other hand, Philippon et al. (2014) used monthly averages (not maxima) of spatially resampled and atmospherically corrected NDVI dataset in their study. The NDVI dataset used in this study is methodologically similar to the one of Philippon et al. (2014) – see section 3.2.2 for its description.

5.3.2 Choice of study areas and study period

McPhaden et al. (2006) claimed that ENSO impacts on all continents as well as all ocean basins. On the other hand, Brands (2017) concluded that ENSO teleconnections to higher than subtropical latitudes are weak or not significant. The volatile nature of ENSO teleconnections to higher latitudes was accounted to too large dependency on the background state of the atmosphere, specifically meaning that internal atmospheric variability might be strong enough to suppress the ENSO signal (Brands, 2017) – see also section 5.4.4. Even McPhaden et al. (2006), who generally advocate studies describing ENSO teleconnections to higher latitudes, admitted that the ENSO teleconnections impact on higher latitudes are less consistent than those to the tropics and the Pacific basin due to regional climate variability modes or weather noise, but still considered them obvious. Hence, despite a number of previous studies describing ENSO impacts in higher latitudes, from mid-latitude China (Zhang and Zhou, 2015) to even Antarctica (Guo et al., 2004), no higher latitude region was included in this paper in order to avoid regions with only uncertain or questionable ENSO influence.

5.3.3 Features specific for vegetation response to ENSO teleconnections

It is important to keep in mind that the vegetation indices have its limits in capturing the vegetation state as well. Jin and Eklundh (2014) cited other authors who had proved that NDVI reliably captures canopy-absorbed fraction of photosynthetically active radiation (FPAR) but has its limits in depicting leaf area index (LAI). Comparing NDVI with a more dynamic Enhanced vegetation index (EVI) in features relevant for this study, NDVI underperformed in areas of high vegetation biomass such as tropical rainforest (Jin and Eklundh, 2014), covering some of this project's study areas. Thus, EVI might be more

appropriate for studying ENSO teleconnections to tropical regions (such as, for instance, Borneo in this study) than NDVI. However, aside Plant phenology index (PPI), no other vegetation index performed better than NDVI in any ecosystem, indicating that NDVI is still an accurate measure of ENSO teleconnections impacting on vegetation.

McPhaden et al. (2006) warned that land use practices might exaggerate observed ENSO impacts. Moreover, a strong ENSO event such as the El Niño of 1997/98 can have long-lasting effect on vegetation state, especially if wildfires are triggered by ENSO-induced drought, leading up to complete change of vegetation cover and a different ecosystem (McPhaden et al., 2006). That would thus limit the potential detection of a typical, recurrent response of the ecosystem to ENSO forcing on the scale of years to decades used in this study. While precipitation is considered critical for depicting teleconnections to crop yields (linked to vegetation greenness), Anderson et al. (2017) noted that it would be wrong to completely dismiss the role of temperature despite relatively low correlations between maximum temperature and crop yields over longer time series, because the relation between the two factors is strongly nonlinear. This project did not test the relations between precipitation/temperature and vegetation, but some of the correlations between the climate variables and NDVI anomalies agreed in sign of the expected ENSO impact (see section 4.1). Moreover, in their study focusing on Americas, Anderson et al. (2017) proved that anomalous crop yields were historically in line with life cycles of ENSO teleconnections. That does not only show the relevance of ENSO teleconnection research but allows assuming that impacts of ENSO teleconnections are visible on the vegetation state even in agricultural areas where irrigation is common.

The contrast in variability of the obtained correlation coefficients for NDVI and the climate variables can be explained by the mosaic of various land cover types that creates a way more differentiated field of NDVI values than the more continuous fields of the climate variables. These differences were, however, smaller if the overall correlation was stronger. It may point to a strength of the method used here, i.e. correlating the standardized anomalies (z-scores) for every grid cell, because those standardized anomalies are able to capture individual variations in the grid cells, which were, due to not a very long study period of this study and their relatively big size, assumed to be representing the same prevailing ecosystem/land cover class over the whole period spanning over this study. However, since practices in agriculture used to adapt and/or mitigate the ENSO impact as predicted by available ENSO forecasts include a change of crop type (Keil et al., 2008), such can possibly lead to anomalous values in the time series of the vegetation indices for the respective grid cells. If such an advanced “ENSO management” was performed in the study areas in the period covered by this paper, it inherently affected the results presented here.

Similarly, soil types and local climatology (different climate characteristics) were expected to be stable during the study area. Anderson et al. (2017) underlined the importance of the underlying seasonal cycle and local climatology because while, for instance, ENSO-driven

positive rainfall anomaly might be profitable for the vegetation in usually dry period, it may be undesirable in water-rich periods.

5.3.4 Role of other climate phenomena

ENSO teleconnections can be constrained by other climate and weather phenomena, which can significantly strengthen or weaken the ENSO signal. Brands (2017) mentioned the study of Hersbach et al. (2015) who named, for instance, aerosols, solar activity, sea ice cover or SSTs in other ocean basins as such modulators. Sterl et al. (2007) explain that the ENSO-independent climate processes operate on different timescales and account for varied strength of long-term ENSO teleconnections gained in observations for a specific region. Other climate phenomena than ENSO accompanied by teleconnections which might need to be taken into account include Interdecadal Pacific Oscillation (IPO) (Cai et al., 2015a) or alternatively Pacific Decadal Oscillation (PDO) (Yeh et al., 2018) since these contribute to atmospheric circulation anomalies or longitudinally alter the center of atmospheric convection in equatorial Pacific. Thanks to their long frequency times, they can as well modulate ENSO teleconnection on the timescales of decades – it is IPO/PDO to which Yeh et al. (2018) ascribed the westward shift of anomaly centers during ENSO events in equatorial Pacific in 21st century compared to the previous century. Since this project only covered the 21st century, it is possible that this interplay between climate and circulation phenomena might be responsible for the disparity between some of the results of this study and other papers which draw their conclusions from longer time series spanning back to 20th century.

Another prominent example of a climate phenomenon affecting ENSO teleconnections is the interplay between ENSO and Indian Ocean Dipole in 1997/98, with the former developed into a very strong El Niño, the latter being in its extreme positive phase, resulting in catastrophic impacts of ENSO teleconnections on Indian subcontinent (Cai et al., 2015a). Yeh et al. (2018) reminded that other ocean basins than tropical Pacific, particularly the northern portions of the Pacific and the Atlantic as well as the Indian Ocean, can impact ENSO teleconnections through sea-air interactions over the respective basin.

Most importantly, though, Yeh et al. (2018) underlined that in many cases, ENSO teleconnections represent only a part of the total climate variability over the respective region. This might impact the discrepancies among results of different studies including this one to a very significant extent, especially since this study did not cover a very long period with many ENSO events.

5.3.5 ENSO indicator selection and asymmetry between El Niño and La Niña

Southern oscillation index (SOI), defined as normalized difference in atmospheric sea level pressure (SLP) between Tahiti and Tasmania or outgoing longwave radiation (OLR) from the area of interest (e.g. the central Pacific area) are just a couple of examples of other ENSO state indicators. Nevertheless, the approach based on Pacific SST (used also in this study) exhibits less noise and is thus more reliable as an ENSO indicator (Plisnier et al., 2000). On the contrary, Yeh et al. (2018) argued that OLR might be a better indicator for ENSO

teleconnections than SST based indices because OLR is more directly attached to the atmospheric forcing driving the teleconnections. Ashok et al. (2007) proposed ENSO Modoki index (EMI) in order to account for increased frequency of ENSO Modoki (CP) events since 1980s (Roy et al., 2017). For studies of ENSO impacts on a fixed location, Cai et al. (2015a) then suggest using more than one ENSO index because of proposed non-uniformity among ENSO events. This could be taken as one possible suggestion for future more detailed studies of the kind of this one.

Furthermore, Cai et al. (2015b) even suggested using separate indices for particularly extreme ENSO events, because while the biggest SST anomalies center in the eastern tropical Pacific during extreme El Niño events (then Nino3.4 region is suitable), extreme La Niña events exhibit the coldest SST anomalies in central Pacific, with Nino4 region (5N – 5S, 160E – 150W) being more appropriate. Linking this to the results presented in this paper, the very strong El Niño 2014(5)-16 might thus need a specific ENSO index to calculate its teleconnections comparably to the other ENSO events.

5.3.6 Climate variables selection

Aside precipitation and temperature, Brands (2017) also explored mean SLP and geopotential height at 500hPa as variables depicting ENSO teleconnections. According to Sterl et al. (2007), these two variables are less noisy than especially precipitation and thus more suitable to capture teleconnections. Incorporating them in the analysis was, however, beyond the scope of this project.

5.3.7 Inconsistent results for a region within the study period

Yeh et al. (2018) reminded that the research on ENSO teleconnections impacts is greatly constricted by their own non-linearity and non-stationarity, which even adds to the omnipresent random noise in the atmosphere. Conclusively, results for certain period and certain region might be inconsistent with a longer time series, without contrasting with available knowledge. This offers another possible explanation to the disparity between some of the results presented here and elsewhere. On the other hand, Roy et al. (2017) concluded that the spatial patterns of ENSO impacts remain unchanged for study periods of varying lengths, suggesting stable spatial patterns of ENSO teleconnections, just with possibly altering strength.

6 Conclusions

The study managed to respond to all the intended aims as stated in the introduction, although sometimes in a different way than could be expect with respect to findings of other studies. Firstly, a strong enough relationship between ENSO and climate and vegetation anomalies was found for all the study areas for at least some of the variables tested in at least one of the seasons.

Secondly, there was always delay of at least one season before ENSO teleconnections strongly impacted the study regions, which can be considered the most interesting result of this study. In other words, concurrent ENSO teleconnections were not found strong enough in none of the cases tested, which can be considered the most interesting result of this project. It could also be interpreted as positive news for disaster and risk management connected to ENSO-caused extreme events and their consequences (as mentioned in chapter 1), because it would allow some time to get prepared for such. If such result was confirmed on a larger scale (spatially and possibly also temporarily) than what was the scope of this project, it would mean that simultaneous impacts of ENSO teleconnections would not have to be considered at all.

Thirdly, most of the affected regions showed very similar pattern in terms of the timing of the strongest ENSO teleconnections impact – it typically came in late northern hemisphere spring and early northern hemisphere summer, following an ENSO event peaking the antecedent northern hemisphere winter, but already the preceding northern hemisphere summer ENSO state was usually evidently correlated with the anomalies detected in the following spring and summer. The typical resulting time lag for the strongest detected teleconnections was 10 months for JJA ONI and 4 months for DJF ONI. Thus, the results were similar with respect to the time lag of ENSO teleconnections impact not only for all the study regions, but basically also for all the three variables used, revealing no obvious time lag between impacts on climate and vegetation anomalies.

Conclusively, the most important message of this project could be to highlight the importance to study not just the strength of ENSO teleconnections, but also the time lag in more detail. As mentioned in the paper, not many studies focused on it and in some cases, this study suggested results that go against the assumptions or findings made by other papers about the lagged effect of ENSO teleconnections. Spatially wider, temporally longer and possibly methodologically more advanced studies on the time lag of ENSO teleconnections would shed further light to the complexity of ENSO mechanisms and impacts observed in this thesis.

References

ABDI, A. M., VRIELING, A., YENGOH, G. T., ANYAMBA, A., SEAQUIST, J. W., UMMENHOFER, C. C. & ARDÖ, J. 2016. The El Niño - La Niña cycle and recent trends in supply and demand of net primary productivity in African drylands. *Climatic Change,* 138**,** 111-125.

ADAMS, R. M., HOUSTON, L. L., MCCARL, B. A., TISCAREÑO L, M., MATUS G, J. & WEIHER, R. F. 2003. The benefits to Mexican agriculture of an El Niño-southern oscillation (ENSO) early warning system. *Agricultural and Forest Meteorology,* 115**,** 183-194.

AHLSTRÖM, A., RAUPACH, M. R., SCHURGERS, G., SMITH, B., ARNETH, A., JUNG, M., REICHSTEIN, M., CANADELL, J. G., FRIEDLINGSTEIN, P., JAIN, A. K., KATO, E., POULTER, B., SITCH, S., STOCKER, B. D., VIOVY, N., WANG, Y. P., WILTSHIRE, A., ZAEHLE, S. & ZENG, N. 2015. The dominant role of semi-arid ecosystems in the trend and variability of the land CO2 sink. *Science***,** 895.

AHRENS, D. C. & HENSON, R. 2016. *Meteorology Today. An introduction to Weather, Climate, and the Environment*.

ANDERSON, W., SEAGER, R., CANE, M. & BAETHGEN, W. 2017. Life cycles of agriculturally relevant ENSO teleconnections in North and South America. *International Journal of Climatology,* 37**,** 3297-3318.

ASHOK, K., BEHERA, S. K., RAO, S. A., WENG, H. & YAMAGATA, T. 2007. El Nino Modoki and its possible teleconnection.

BRANDS, S. 2017. Which ENSO teleconnections are robust to internal atmospheric variability? *Geophysical Research Letters,* 44**,** 1483-1493.

CAI, W., SANTOSO, A., GUOJIAN, W., SANG-WOOK, Y., SOON-IL, A., COBB, K. M., COLLINS, M., GUILYARDI, E., FEI-FEI, J., JONG-SEONG, K., LENGAIGNE, M., MCPHADEN, M. J., TAKAHASHI, K., TIMMERMANN, A., VECCHI, G., WATANABE, M. & LIXIN, W. 2015a. ENSO and greenhouse warming. *Nature Climate Change,* 5**,** 849-859.

CAI, W., VAN RENSCH, P., COWAN, T. & HENDON HARRY, H. 2011. Teleconnection Pathways of ENSO and the IOD and the Mechanisms for Impacts on Australian Rainfall. *Journal of Climate,* 24**,** 3910.

CAI, W., WANG, G., SANTOSO, A., MCPHADEN, M. J., WU, L., JIN, F.-F., TIMMERMANN, A., COLLINS, M., VECCHI, G., LENGAIGNE, M., ENGLAND, M. H., DOMMENGET, D., TAKAHASHI, K. & GUILYARDI, E. 2015b. Increased frequency of extreme La Nina events under greenhouse warming. *Nature Climate Change,* 5**,** 132-137.

CIRINO, P. H., FÉRES, J. G., BRAGA, M. J. & REIS, E. 2015. Assessing the Impacts of ENSO-related Weather Effects on the Brazilian Agriculture. *Procedia Economics and Finance,* 24**,** 146-155.

CLIMATE.GOV, N. 2016. *Global Impacts of El Niño and La Niña* [Online]. Available: https://www.climate.gov/news-features/featured-images/global-impacts-el-ni%C3%B1o-and-la-ni%C3%B1a [Accessed].

ERASMI, S., SCHUCKNECHT, A., P. BARBOSA, M. & MATSCHULLAT, J. 2014. Vegetation Greenness in Northeastern Brazil and Its Relation to ENSO Warm Events. *Remote Sensing, Vol 6, Iss 4, Pp 3041-3058 (2014)***,** 3041.

FOROOTAN, E., KHANDU, AWANGE, J. L., SCHUMACHER, M., ANYAH, R. O., VAN DIJK, A. I. J. M. & KUSCHE, J. 2016. Quantifying the impacts of ENSO and IOD on rain gauge and remotely sensed precipitation products over Australia. *Remote Sensing of Environment,* 172**,** 50-66.

GUO, Z., BROMWICH DAVID, H. & HINES KEITH, M. 2004. Modeled Antarctic Precipitation. Part II : ENSO Modulation over West Antarctica. *Journal of Climate,* 17**,** 448.

HANNAH, L. 2015. *Climate Change Biology. [Elektronisk resurs]*, London : Academic Press, 2015

2. ed.

HARRIS, I., JONES, P. D., OSBORN, T. J. & LISTER, D. H. 2014. Updated high-resolution grids of monthly climatic observations - the CRU TS3.10 Dataset. *International Journal of Climatology,* 34**,** 623-642.

HERSBACH, H., PEUBEY, C., SIMMONS, A., BERRISFORD, P., POLI, P. & DEE, D. 2015. ERA-20CM: A twentieth-century atmospheric model ensemble. *Quarterly Journal of the Royal Meteorological Society,* 141**,** 2350-2375.

HURRELL, J. W. & DESER, C. 2009. North Atlantic climate variability: The role of the North Atlantic Oscillation. *Journal of Marine Systems,* 78**,** 28-41.

CHUVIECO, E. 2016. *Fundamentals of satellite remote sensing : an environmental approach*, Boca Raton : CRC Press.

JIN, H. & EKLUNDH, L. 2014. A physically based vegetation index for improved monitoring of plant phenology. *Remote Sensing of Environment,* 152**,** 512-525.

KEIL, A., ZELLER, M., WIDA, A., SANIM, B. & BIRNER, R. 2008. What determines farmers' resilience towards ENSO-related drought? An empirical assessment in Central Sulawesi, Indonesia. *Climatic Change,* 86**,** 291-307.

MCPHADEN, M. J., ZEBIAK, S. E. & GLANTZ, M. H. 2006. ENSO as an Integrating Concept in Earth Science. *Science***,** 1740.

PHILIPPON, N., MARTINY, N., CAMBERLIN, P., HOFFMAN, M. T. & GOND, V. 2014. Timing and Patterns of the ENSO Signal in Africa over the Last 30 Years: Insights from Normalized Difference Vegetation Index Data. *Journal of Climate,* 27**,** 2509-2532.

PLISNIER, P. D., SERNEELS, S. & LAMBIN, E. F. 2000. Impact of ENSO on East African Ecosystems: A Multivariate Analysis Based on Climate and Remote Sensing Data. *Global Ecology and Biogeography***,** 481.

ROPELEWSKI, C. F. & HALPERT, M. S. 1987. Global and regional scale precipitation patterns associated with El NiñoSouthern oscillation. *Monthly Weather Review,* 115**,** 1606-1626.

ROY, I., TEDESCHI, R. G. & COLLINS, M. 2017. ENSO teleconnections to the Indian summer monsoon in observations and models. *International Journal of Climatology,* 37**,** 1794-1813.

SONG, L., CHEN, S., CHEN, W. & CHEN, X. 2017. Distinct impacts of two types of La Niña events on Australian summer rainfall. *International Journal of Climatology,* 37**,** 2532-2544.

STERL, A., VAN OLDENBORGH, G. J., HAZELEGER, W. & BURGERS, G. 2007. On the robustness of ENSO teleconnections. *Climate Dynamics,* 29**,** 468-485.

TAKAHASHI, K. 2015. *One forecaster's view on extreme El Niño in the eastern Pacific* [Online]. NOAA. Available: https://www.climate.gov/news-features/blogs/enso/one-forecaster%E2%80%99s-view-extreme-el-ni%C3%B1o-eastern-pacific [Accessed].

TRENBERTH, K. E. 1997a. The Definition of El Niño. *Bulletin of the American Meteorological Society,* 78**,** 2771.

TRENBERTH, K. E. 1997b. Short-Term Climate Variations : Recent Accomplishments and Issues for Future Progress. *Bulletin of the American Meteorological Society,* 78**,** 1081.

TURNER, J. 2004. The El Niño-Southern Oscillation and Antarctica. *International Journal of Climatology,* 24**,** 1-31.

WANG, C. & FIEDLER, P. C. 2006. ENSO variability and the eastern tropical Pacific: A review. *Progress in Oceanography,* 69**,** 239-266.
WANG, G., CAI, W., GAN, B., WU, L., LIN, X., CHEN, Z., SANTOSO, A. & MCPHADEN, M. J. 2017. Continued increase of extreme El Ninõ frequency long after 1.5 C warming stabilization. *Nature Climate Change,* 7**,** 568-572.
WOLTER, K. & TIMLIN, M. S. 2011. El Niño/Southern Oscillation behaviour since 1871 as diagnosed in an extended multivariate ENSO index (MEI.ext). *International Journal of Climatology,* 31**,** 1074.
YEH, S. W., CAI, W., MIN, S. K., KUG, J. S., MCPHADEN, M. J., DOMMENGET, D., DEWITTE, B., COLLINS, M., ASHOK, K., AN, S. I. & YIM, B. Y. 2018. ENSO Atmospheric Teleconnections and Their Response to Greenhouse Gas Forcing. *Reviews of Geophysics,* 56**,** 185-206.
ZHANG, L. & ZHOU, T. 2015. Drought over East Asia: a review. *Journal of Climate,* 28**,** 3375-3399.

Appendix

Fig. A1-A8 show the study areas on maps.

Retrieved as basemaps from ArcMap. Source data for the maps: National Geographic, Esri, Garmin, HERE, UNEP-WCMC, USGS, NASA, ESA, METI, NRCAN, GEBCO, NOAA, increment P Corp.

Fig. A1– Study area *Africa* in its spatial limits

Fig. A2 – Study area *Brazil* in its spatial limits

Fig. A3 – Study area *Gulf of Mexico* in its spatial limits

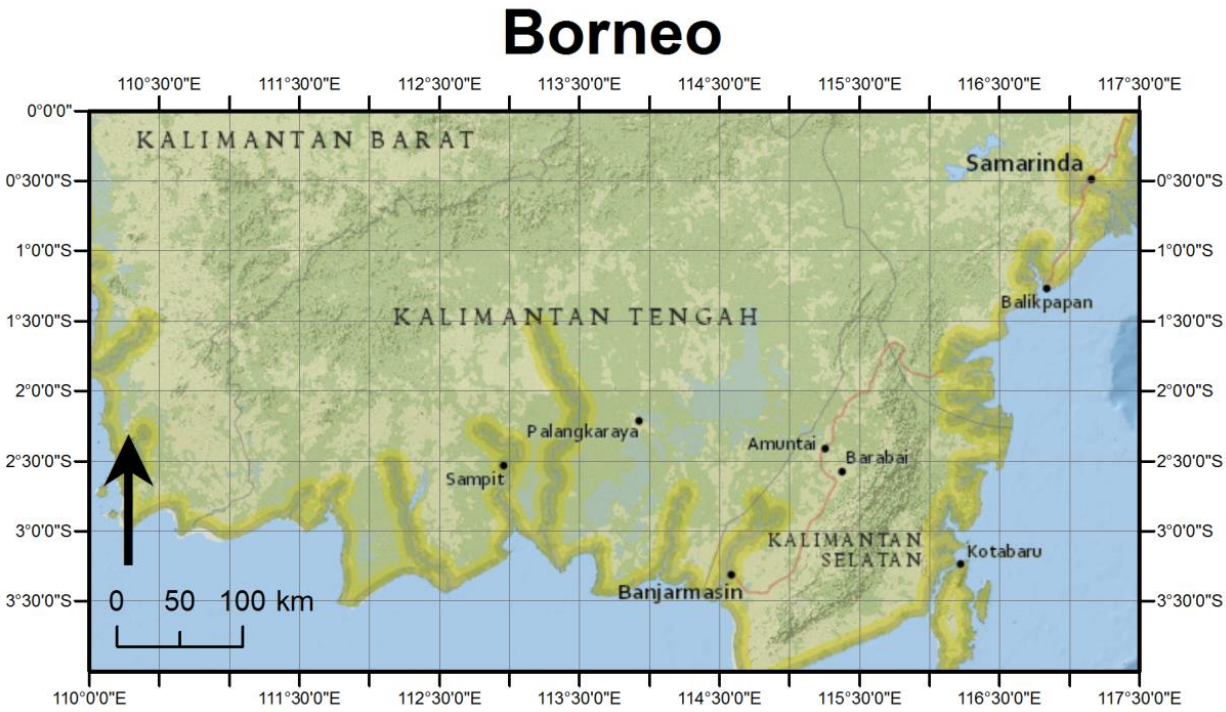

Fig. A4 – Study area *Borneo* in its spatial limits

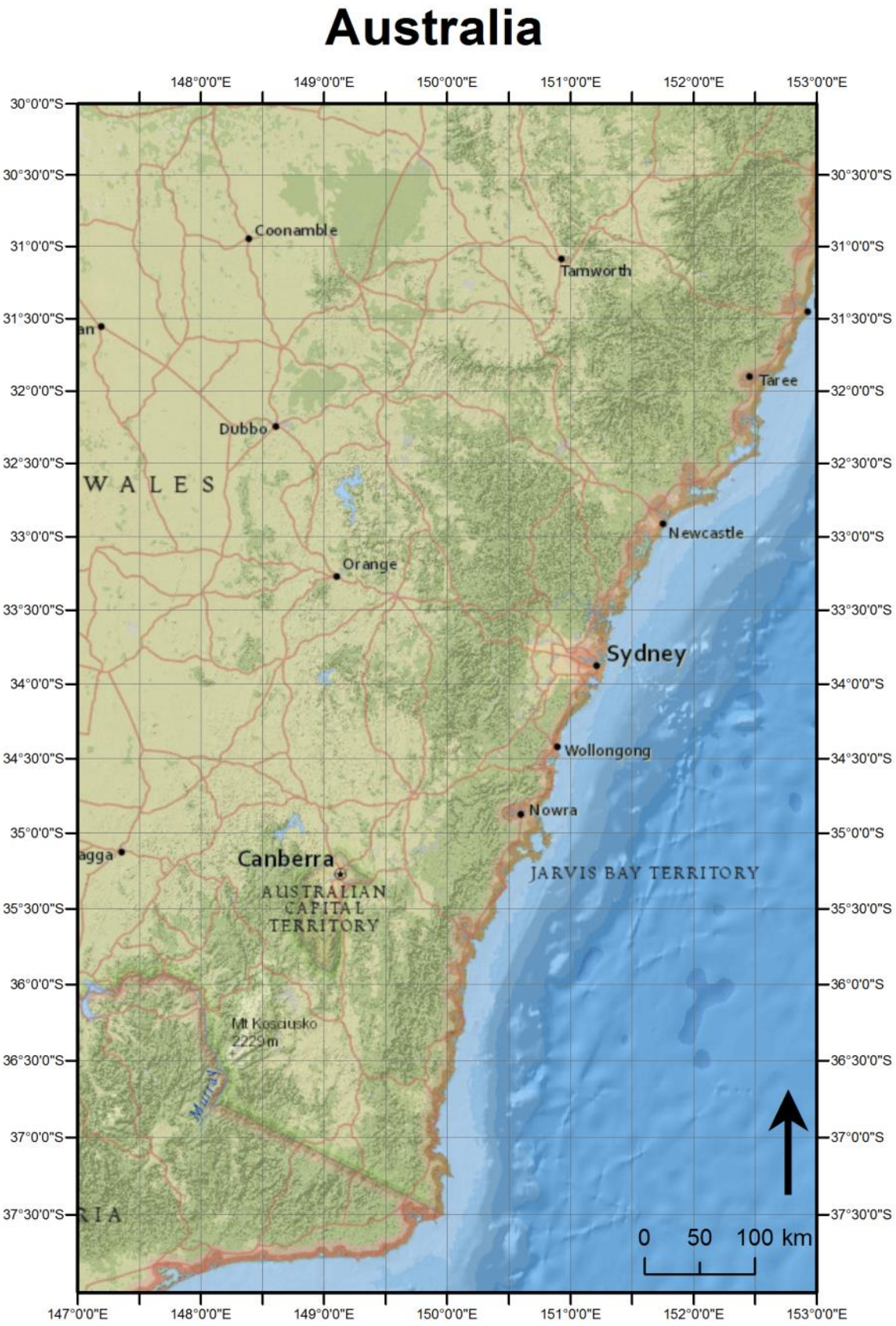

Fig. A5 – Study area *Southern hemisphereia* in its spatial limits

Fig. A6 – Study area *Florida* in its spatial limits

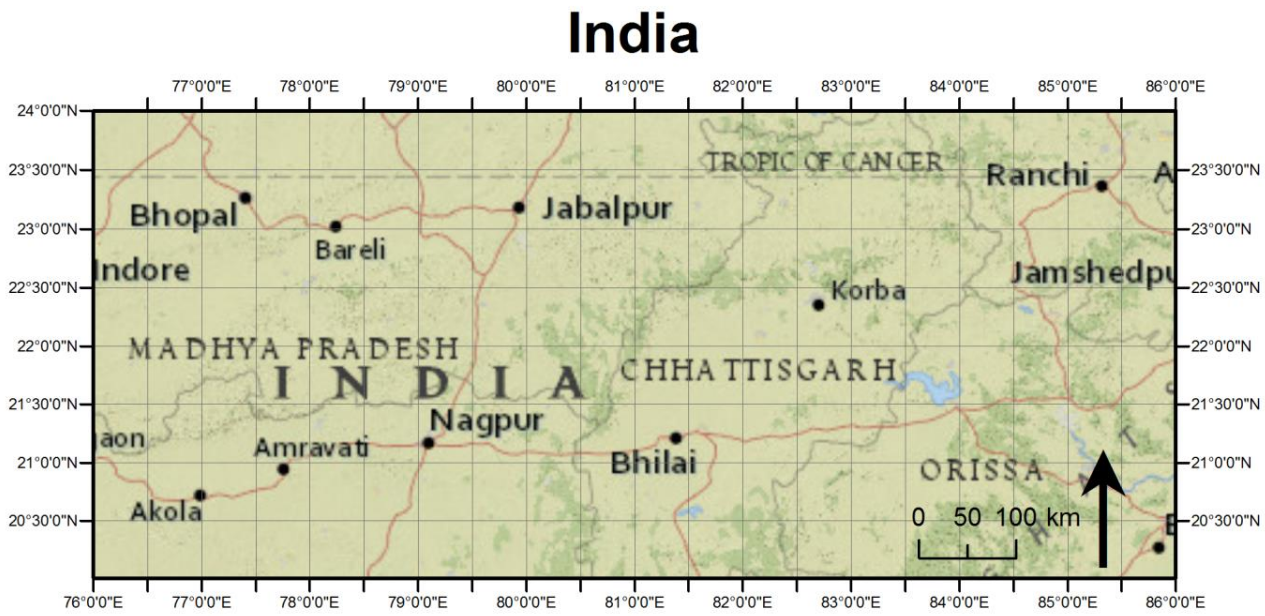

Fig. A7 – Study area *India* in its spatial limits

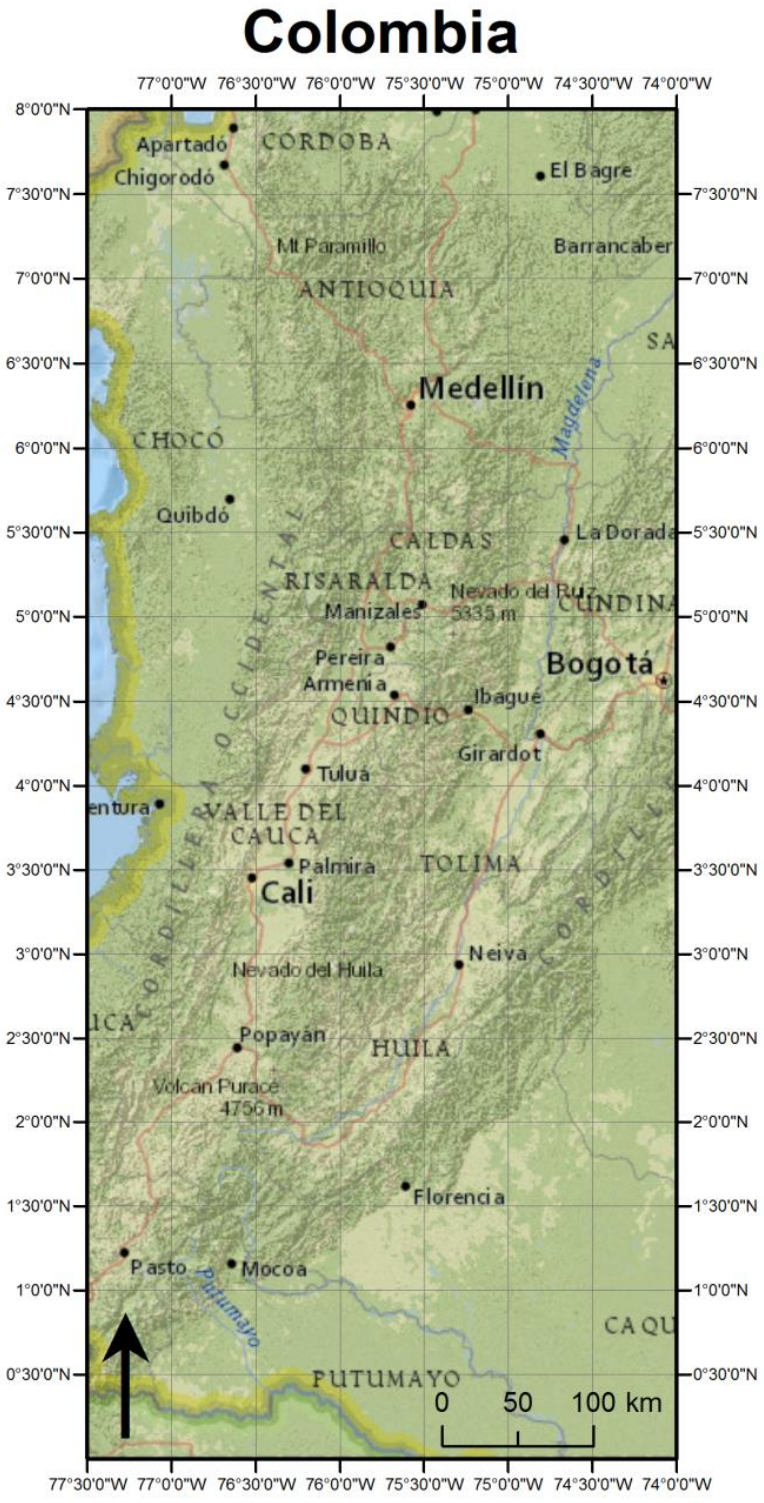

Fig. A8 – Study area *Colombia* in its spatial limits